UCID-20744

Atomic Physics and Non-Equilibrium Plasmas

Jon C. Weisheit

April 25, 1986

Printed in the United States of America
Available from
National Technical Information Service
U.S. Department of Commerce
5285 Port Royal Road
Springfield, VA 22161

Price Code	Page Range
A01	Microfiche
Papercopy Prices	
A02	001-050
A03	051-100
A04	101-200
A05	201-300
A06	301-400
A07	401-500
A08	501-600
A09	601

ATOMIC PHYSICS AND NON-EQUILIBRIUM PLASMAS

Jon C. Weisheit
Physics Department

The purpose of these three lectures is to provide a fairly general introduction to the atomic phenomena that play an important role in the behavior of non-equilibrium plasmas. Because I must present many topics, no one of them can get much attention.

First, let me give some working definitions of terms used above:

atomic physics: structure of atoms (usually highly ionized); collisional and radiative interactions among electrons, ions, and photons; ionization equilibria; and spectral line shapes.

non-equilibrium plasma: a plasma of electrons and ions, in which the atomic level populations are not generally given by classical (Maxwell-Boltzman) or quantum (Fermi-Dirac) statistics. However, particle velocity distributions are assumed to be statistical, being characterized by a well-defined temperature, T.

I will invariably assume that electrons and ions have the same temperature, but the generalization of my comments to cases where $T_e \neq T_i$ is quite straightforward. Generalization to cases where T is undefined certainly is messy numerically, but again is straightforward in principle. And finally, I shall make no restrictive assumption about the radiation field -- it may or may not have a simple characterization.

Also, I want to recommend a few texts to you, so that you can follow up my comments with much more detailed reading, if a particular subject interests you.

1. H. A. Bethe and E. E. Salpeter, Quantum Mechanics of One- and Two-Electron Atoms (1957).

2. N. F. Mott and H. S. W. Massey, The Theory of Atomic Collisions (1965).

3. H. A. Bethe and R. Jakiw, Intermediate Quantum Mechanics (1968).

4. I. I. Sobelman, Atomic Spectra and Radiative Transitions (1979).

5. I. I. Sobelman, L. A. Vainshtein, and E. A. Yukov, Excitation of Atoms and Broadening of Spectral Lines (1981).

6. R. D. Cowan, The Theory of Atomic Structure and Spectra (1981).

With these prefatory remarks out of the way, let's turn to the subject at hand.

LECTURE #2: ATOMIC STRUCTURE

This first lecture discusses atomic structure – primarily theory, but also some experimental data. Our topical order is:

1. Non–relativistic one–electron atom
2. Relativistic one–electron atom
3. Non–relativistic many–electron atom
   a. Central field approximations
   b. Configurations and wavefunctions
   c. Angular momentum
4. Relativistic many–electron atom

The Hydrogen Atom (Non–Relativistic)

The purpose here is not to bore you with a discussion of associated Laguerre polynomials; rather it is to remind you of some basic facts, and to introduce notation we will often need later.

The time independent Schrödinger equation for hydrogen is

$$\left[-\frac{\hbar^2}{2\mu} \nabla^2 + V(r) - E_\Gamma \right] \psi_\Gamma(\vec{r}) = 0 \ , \tag{2.1}$$

where the potential energy is

$$V(r) = -\frac{Ze^2}{r} \ , \tag{2.2}$$

Ze is the charge of the nucleus, $\mu \sim m_e$ is the reduced mass, and E_Γ is the eigenvalue of the quantum state "Γ". As you probably recall, three quantum numbers are needed to completely label the solution $\psi(r)$:

$$\Gamma \rightarrow \begin{cases} n = \text{principal quantum number} \\ \ell = \text{orbital angular momentum quantum number} \\ m_\ell = \text{azimuthal (or projection) quantum number} \end{cases}$$

Their allowed values are:

$$n = 1, 2, 3, \ldots ; \ \ell = 0, 1, \ldots, n-1 \ ; \ m_\ell = -\ell, -\ell+1, \ldots, \ell-1, \ell. \tag{2.3}$$

In spherical polar coordinates we write

$$\psi_\Gamma(\vec{r}) = \psi_{n\ell m_\ell}(\vec{r}) = \frac{1}{r} P_{n\ell}(r)\, Y_{\ell m_\ell}(\hat{r}) \ , \tag{2.4}$$

where the spherical harmonic Y is a function of the spherical polar angles $(\theta, \varphi) = (\hat{r})$ of $\vec{r}$, and where the radial function is the solution of the second order equation (cf Bethe and Salpeter)

$$P''_{n\ell} + \left[\frac{2\mu E_\Gamma}{\hbar^2} + \frac{2\mu Ze^2}{\hbar^2 r} - \frac{\ell(\ell+1)}{r^2}\right] P_{n\ell} = 0 \ . \tag{2.5a}$$

As in other fields of physics, a particularly convenient set of units suggests itself for atomic physics calculations. We often will use the following ones:

charge:	the proton charge,	$e = 4.80325 \times 10^{-10}$ esu
mass:	the electron mass,	$m_e = 9.10956 \times 10^{-28}$ g
length:	Bohr radius,	$a_o = \hbar^2/m_e e^2 = 0.529177$ Å
energy:	atomic unit,	e^2/a_o = 2Rydberg = 2(13.60583 eV)

{i.e., we put $e = \hbar = m_e = 1$.} For most calculations one can approximate the reduced mass as m_e, and then, for example, the radial equation takes the form

$$P''_{n\ell}(r) + [E_\Gamma + 2Z/r - \ell(\ell+1)/r^2]\, P_{n\ell}(r) = 0 \ . \tag{2.5b}$$

Henceforth, if units are not mentioned, atomic units have been adopted.

Some Properties of the Hydrogen Atom

Although the solution of Eq. (2.1) requires us to define the three quantum numbers (n, ℓ, m_ℓ), the hydrogenic engenvalues depend only on n:

$$E_\Gamma = -\frac{Z^2}{2n^2} \ . \tag{2.6}$$

There are $(2\ell+1)$ possible magnetic substates for each ℓ–value and n possible angular momentum states for each principal quantum number. We can trivially compute the number of degenerate eigenstates to be

$$g_n = \sum_{\ell=0}^{n-1} (2\ell+1) = n^2 \ . \tag{2.7}$$

Now, the spherical harmonic functions, which are the eigenfunctions of the angular momentum operators ℓ^2 and ℓ_z, are orthonormal,

$$\langle Y_{\ell m_\ell} | Y_{\ell' m'_\ell} \rangle = \delta_{\ell\ell'} \delta_{m_\ell m'_\ell} \quad , \tag{2.8}$$

but the radial functions satisfy only the incomplete orthogonality condition

$$\langle \frac{1}{r} P_{n\ell} | \frac{1}{r} P_{n'\ell} \rangle = \delta_{nn'} . \tag{2.9}$$

One other important property of the eigenfunction $\Psi(\vec{r})$ is its <u>parity</u>. Recall that the parity operation Ω corresponds here to a reflection through the origin, viz. $\vec{r} \to -\vec{r}$. We have, therefore,

$$\Omega \psi(\vec{r}) = \frac{1}{r} P_{n\ell}(r)\, \Omega\, Y_{\ell m}(\hat{r}) = (-1)^\ell \psi(\vec{r}) \ . \tag{2.10}$$

States with ℓ=0, 2, . . . , etc. are called even parity states, while those with odd ℓ–values are called odd parity states.

So much for theory. What are the facts? In this instance, the "facts" are spectroscopic data that reveal the wavelengths $\lambda_{\Gamma\Gamma'}$, corresponding to the $\Gamma \to \Gamma'$ transitions:

$$\frac{1}{\lambda_{\Gamma\Gamma'}} = \frac{Z^2\alpha}{4\pi a_o} \left| \frac{1}{n'^2} - \frac{1}{n^2} \right| , \tag{2.11}$$

with $\alpha = e^2/\hbar c \simeq 1/137$ being the fine–structure constant. One example is reproduced here, the 4686Å line of He^+, corresponding to the (n=4) → (n'=3) transition. Evidently, our physics is incomplete, since Eq. (2.11) predicts a single transition wavelength, independent of the values of ℓ and ℓ', and m_ℓ and m'_ℓ.

What are missing are the complications introduced by relativistic effects, such as $m_e = m_e(v)$, and the existence of electron spin. By using first–order perturbation theory ($v/c \ll 1$ in hydrogen), Sommerfeld, Uhlenbeck and Goudsmit, and Thomas all made contributions to extend Schrödinger's theory and obtain satisfactory agreement with experimental data available at that time. However, the perturbative treatment is inadequate for heavy atoms, wherein there are bound electrons with speeds $v \sim Z\alpha c$. Further, not all the terms in the relativistic Hamiltonian have classical counterparts. Therefore, instead of tracing the historical development of the theory of fine structure, we shall obtain the correct formulae from Dirac's (1928) relativistic wave equation for spin – 1/2 particles.

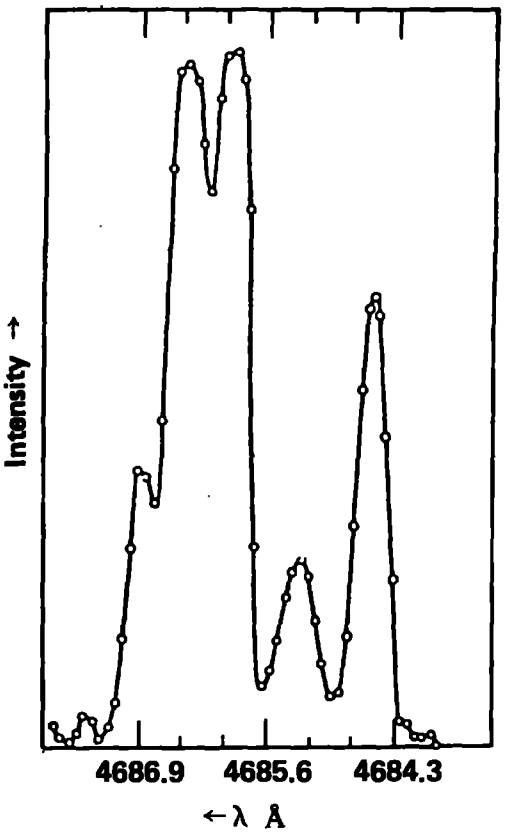

FIG. 2.1. The He^+ 4686Å line at high resolution.

The Dirac Equation for Free Particles of Spin 1/2

As a preliminary comment, we note that the existence of spin angular momentum $\vec{s}\hbar$ for the electron, with just the two eigenvalues $m_s = \pm 1/2$ for its projection onto a quantization axis, had been postulated in 1925, before Dirac's work. A convenient choice of basis functions for the spin operator s is $\binom{1}{0}$ and $\binom{0}{1}$; in this representation we have

$$s^2 = \begin{pmatrix} 3/4 & 0 \\ 0 & 3/4 \end{pmatrix}, \; s_x = \begin{pmatrix} 0 & 1/2 \\ 1/2 & 0 \end{pmatrix}, \; s_y = \begin{pmatrix} 0 & -i/2 \\ -i/2 & 0 \end{pmatrix}, \; s_z = \begin{pmatrix} 1/2 & 0 \\ 0 & 1/2 \end{pmatrix} .$$

These matrices play an important role in the Dirac theory.

It is readily apparent that the Schrödinger equation (SE) is not invariant under a Lorentz transformation, since space and time derivatives are not of the same order. An obvious relativistic analogue of the SE is obtainable from the energy formula for a particle of rest mass m_o,

$$E^2 = p^2c^2 + m_o^2c^4 \tag{2.13}$$

plus the correspondence principle, viz.,

$$E \rightarrow -\frac{\hbar}{i}\frac{\partial}{\partial t}\,;\; p_k \rightarrow \frac{\hbar}{i}\frac{\partial}{\partial x_k}\,. \tag{2.14}$$

This gives the Klein–Gordon (KG) equation,

$$[\nabla^2 - \frac{1}{c^2}\frac{\partial^2}{\partial t^2}]\,\Psi = (\frac{m_o^2 c^2}{\hbar^2})\,\Psi\,. \tag{2.15}$$

Because of problems with specification of $\frac{\partial \Psi}{\partial t}$ at some initial time, and the possibility of negative probability density, the KG equation was ignored at first.*

As you may remember, Dirac's solution to these difficulties was to formally extract the square root of Eq. (2.13), by writing

$$E/c = +\sqrt{\sum_{k=1}^{3} p_k^2 + m_o^2 c^2} \equiv \sum_k \alpha_k p_k + \beta m_o c \tag{2.16}$$

The four quantites $\{\alpha_1,\alpha_2,\alpha_3,\beta\}$ clearly are not just numbers, but they do satisfy an algebra whose rules are gotten by squaring Eq. (2.16) and requiring the result to be the same as Eq. (2.13). When this is done, and the correspondence principle invoked again, one has the Dirac equation for a free particle:

$$[\frac{\hbar}{i}\frac{\partial}{\partial t} + \frac{c\hbar}{i}\sum_{k=1}^{3}\alpha_k\frac{\partial}{\partial x_k} + \beta m_o c^2]\;\Psi(\vec{r},t) = 0\,. \tag{2.17}$$

Of course, what we have at this point is of no real value, since we cannot do any calculations without knowing what β and the α_k's are.

Details:

We can employ the relations used to obtain Eq. (2.17), and then perform a series of manipulations in order to be able to make the following statements (cf. Bethe and Jakiw):

1. The four operators $\gamma_k = -i\beta\alpha_k$ (k=1,2,3) and $\gamma_4 = \beta$ anticommute, viz $\gamma_\mu\gamma_\nu + \gamma_\nu\gamma_\mu = 2\delta_{\mu\nu}$.
2. The matrix representation of these four operators must have a dimension N that is even.

*It was revived a few years later by Pauli and Weisskopf, who reinterpreted it. However, it is not satisfactory for spin–1/2 particles, as it does not lead to agreement with spectroscopic data.

3. A representation of dimension N=2 can accomodate only 3 anticommuting operators.
4. Therefore, N=4 is the simplest representation of the γ_μ.

Although there are innumerable equivalent representations the one adopted universally is

$$\alpha = \begin{pmatrix} 0 & \sigma \\ \sigma & 0 \end{pmatrix} , \quad \beta = \begin{pmatrix} I & 0 \\ 0 & -I \end{pmatrix} , \tag{2.18}$$

where I is the 2 x 2 identity matrix and $\sigma = 2s$, with s being the spin matrix of Eq. (2.12); σ is usually called the Pauli matrix.

Because the Dirac operators are of dimension 4, the relativistic wavefunction $\Psi(r,t)$ must have 4 components. For reasons to become apparent soon, we first write Ψ in terms of two, 2–component vectors:

$$\Psi(\vec{r},t) = \begin{bmatrix} \Psi_A(\vec{r},t) \\ \Psi_B(\vec{r},t) \end{bmatrix} . \tag{2.19}$$

For a free particle we can put $\Psi(\vec{r},t) = \psi(\vec{r})e^{-iEt/\hbar}$, and then obtain the pair of equations

$$c\sigma\cdot\vec{p}\,\psi_B(\vec{r}) + (m_o c^2 - E)\psi_A(\vec{r}) = 0 ,$$

$$c\sigma\cdot\vec{p}\,\psi_A(\vec{r}) - (m_o c^2 + E)\,\psi_B(\vec{r}) = 0 , \tag{2.20}$$

If we choose a frame in which $\vec{p} = 0$, then ψ_A is the eigenfunction corresponding to positive energy solutions, and ψ_B to negative energy solutions. (We will not discuss the "positron sea" here.) This accounts for two of the four components.

The existence of two more components, still with the same energy (remember, this is a <u>free</u> particle), suggests that there is some observable which is a constant of the motion, in addition to $\vec{p}$:

$$\frac{dp_x}{dt} = \frac{i}{\hbar}[H, p_x] = 0 . \tag{2.21}$$

Following our classical intuition, we guess first that it is the orbital angular momentum $\vec{\ell}$. But one can directly calculate

$$\frac{d\vec{\ell}}{dt} = \frac{i}{h}[H, \vec{\ell}] = c\,\alpha \times \vec{p}\ , \tag{2.22}$$

which, in general, is not identically zero! Either we must forsake conservation of angular momentum, or we must generalize our definition, adding to $\vec{\ell}$ some quantity $\vec{\Sigma}$ whose time derivative is the negative of Eq. (2.22). This requirement, plus the general property of angular momentum operators, $\Sigma \times \Sigma = i\,\Sigma$, can be satisfied by putting

$$\Sigma = \begin{pmatrix} s & 0 \\ 0 & s \end{pmatrix}\ . \tag{2.23}$$

Thus it is not $\vec{\ell}$, but rather

$$\vec{j} \equiv \vec{\ell} + \vec{s} = \vec{\ell} + \frac{\vec{1}}{2}\ , \tag{2.24}$$

which is conserved for a spin–1/2 particle.

Finally, if we inspect the eigenvalue equation

$$\Sigma_z\, \Psi(\vec{r},t) = \begin{pmatrix} s_z & 0 \\ 0 & s_z \end{pmatrix} \Psi(\vec{r},t) = \frac{1}{2} \begin{bmatrix} +\Psi_1 \\ -\Psi_2 \\ +\Psi_3 \\ -\Psi_4 \end{bmatrix}\ , \tag{2.25}$$

we see that the other two components of Ψ are needed to represent different spin states of a Dirac particle.

Dirac Particle in an External Field

To treat the relativistic effects of an electromagnetic field, including the Coulomb field of the nucleus, we begin with the time–independent free–particle Dirac equation,

$$(H - E)\psi(\vec{r}) = (c\,\alpha \cdot \vec{p} + \beta m_o c^2 - E)\psi(\vec{r}) = 0\ , \tag{2.26}$$

and make the familiar replacements for a charge q,

$$\vec{p} \to \pi = \vec{p} - q\vec{A}/c\ ,\ E \to E - q\phi\ , \tag{2.27}$$

involving $\vec{A}$ and ϕ, the vector and scalar potentials of the field. These substitutions must be justified by comparison with experiment; fortunately, the agreement is excellent.

The exact solution of the Dirac equation leads to two coupled (1st order) differential equations for the radial parts of ψ_A and ψ_B. Instead of discussing these equations, we find it more instructive to summarize the analysis of Pauli, who obtained an approximate equation for the positive–energy solution ψ_A, in the limit that $E - m_o c^2 << m_o c^2$. It turns out that the Pauli equation is exact to order $(v/c)^2$.

Suppose we replace, in Eq. (2.20), the term $E+m_o c^2$ by $2m_o c^2$. Then,

$$\psi_B = \frac{\sigma\cdot\vec{p}}{2m_o c^2}\,\psi_A \sim \left(\frac{v}{c}\right)\psi_A \ . \tag{2.28}$$

The basis of Pauli's approximation is to insert this result into the companion equation, getting an equation for just ψ_A:

$$\left[\frac{(c\,\sigma\cdot\vec{p})\,(c\,\sigma\cdot\vec{p})}{2m_o c^2} + (m_o c^2 - E)\right]\psi_A = 0 \ . \tag{2.29}$$

If we stop here, and use the correspondences of Eq. (2.27), we obtain the non–relativistic Pauli equation,

$$\left[\,(m_o c^2 - E + q\phi) + \frac{1}{2m_o}(\vec{p} - q\vec{A}/c)^2 - \frac{q\hbar}{2m_o c}\,\sigma\cdot\,(\vec{\nabla}\times\vec{A})\,\right]\psi_A = 0 \ . \tag{2.30}$$

Evidently, at this stage, the two components of ψ_A differ only because of the (small) spin–dependent term, which represents the interaction of a magnetic field and a magnetic dipole moment,

$$\vec{\mu} = \frac{q\hbar}{2m_o c}\,\vec{\sigma} \ , \tag{2.31}$$

This term causes part of the normal Zeeman effect.

The relativistic Pauli equation is gotton by performing another iteration, viz.

1. Solve Eq. (2.30) for ψ_A;
2. Substitute this into Eq. (2.28) and obtain an improved ψ_B; and
3. Use improved ψ_B to get new ψ_A.

A lot of algebra is necessary; the result is an equation with the Hamiltonian

$$H\,\{\text{Pauli}\} = H\{\text{n–rel.Pauli}\} + H\{\text{rel. Pauli}\} \ , \tag{2.32}$$

where the non–relativistic part is the Hamiltonian of Eq. (2.30), and where the relativistic correction contains five terms. They are:

$$-\frac{1}{2m_o c^2}(m_o c^2 - E + q\phi)^2 , \quad : \text{(variation of mass with velocity)} , \tag{2.33a}$$

$$-\frac{q}{m_o c}\vec{A}\cdot\vec{p} , \quad : \text{(source of Larmor precision; the rest of normal Zeeman effect)} , \tag{2.33b}$$

$$+\frac{q^2 A^2}{2m_o c^2} \quad : \text{(quadratic Zeeman effect)} , \tag{2.33c}$$

$$+\frac{i q \hbar}{(2m_o c)^2}[(-\vec{\nabla}\phi)\cdot\vec{p}] , \quad : \text{(Darwin term; interaction of electric field and effective electric dipole } d_{eff} = -iq\hbar p/(2m_o c)^2\text{)}, \tag{2.33d}$$

$$-\frac{q\hbar}{(2m_o c)^2}\vec{\sigma}\cdot[(-\vec{\nabla}\phi)\times\vec{p}] \quad : \text{(interaction of moving charge and effective magnetic field } -(\nabla\phi)\times p\text{; this term yields spin–orbit energy in atoms).} \tag{2.33e}$$

None of the first three terms involve the particle spin $\vec{\sigma}$, and all can be obtained from classical analogs ($\hbar \to 0$).

The Relativistic Hydrogen Atom

For the H–atom problem, we must put

$$q = -e, \; m_o = m_e, \; \phi = \frac{Ze}{r} , \quad \vec{A} = 0 .$$

Then, for instance, the spin–orbit interaction of Eq. (2.33e) becomes (atomic units)

$$H_{so} = -\frac{\alpha^2}{2}\frac{1}{r}\frac{d\phi}{dr}(\vec{\sigma}\cdot\vec{\ell}) = +\frac{Z\alpha^2}{2}\frac{1}{r^3}(\vec{\sigma}\cdot\vec{\ell}) . \tag{2.34}$$

If we use perturbation theory to evaluate the relativistic and spin–dependent terms in the Pauli Hamiltonian, the result is a first–order corrected eigenvalue (atomic units),

$$E_{n\ell j}^{(1)} = E_n^{(0)} - \frac{\alpha^2 Z^4}{2n^3}\left(\frac{1}{j+1/2} - \frac{3}{4n}\right). \tag{2.35}$$

Apparently, all states having the same values of j and n are degenerate (viz. $E^{(1)}$ is independent of ℓ, m_ℓ, m_s). This is even true for the exact result,

$$E_{n\ell j} = \frac{1}{\alpha^2}\left\{1 + \frac{(Z\alpha)^2}{\left[n - (j+1/2) + \sqrt{(j+1/2)^2 - (Z\alpha)^2}\right]^2}\right\}^{-1/2} - \frac{1}{\alpha^2}, \qquad (2.36)$$

which agrees with Eq. (2.35) through terms of order $(Z\alpha)^2$. Quantum electrodynamic effects (e.g., Lamb shift) are of order $(Z\alpha)^4$, and since these are not part of the Dirac formalism, it doesn't make much sense to expand the exact result to this next order. The number of (ℓ, m_ℓ, m_s) combinations that can be associated with a given (nj) pair is $g_{nj} = 2j+1$. Since j takes on values from 1/2 to n–1/2, the total statistical weight of all states having a given n is $g_n = 2n^2$. This is twice what is given by Eq. (2.7) because now we also have two spin states, $m_s = \pm 1/2$, for each $(n\ell m_\ell)$ possibility.

One reason we have spent so much time on hydrogen and these small corrections to its eigenvalue spectrum is that, as Z gets large, the corrections no longer are small. Some examples of this fact are given in the accompanying table and figure. The second reason is that our concepts and equations for treating many–electron atoms are extensions of the one–electron–atom formalism.

TABLE 2.1. Hydrogenic energy data [from G. W. Erickson, J. Chem. Phys. Ref. Data, 6, 831 (1977)].

Z	$E(2p_{3/2})$	$\Delta E(2p_{3/2}, 2p_{1/2})$	$\Delta E(2s_{1/2}, 2p_{1/2})$
1	–3.40 eV	4.52_{-5} eV	4.37_{-6} eV
30	–3070.	37.9	0.960
100	–35200.	6920.	71.9

Note: the $(2p_{3/2}, 2p_{1/2})$ splitting is due to fine–structure terms, while the $(2p_{1/2}, 2s_{1/2})$ splitting is due to radiative corrections (Lamb shift).

Many–Electron Atom (non–relativistic)

Most atomic processes we are interested in involve the transition of a single bound electron from one quantum state to another. For this reason, it is particularly convenient to describe an N–electron atomic wave function as a product of 1–electron orbitals ψ_i:

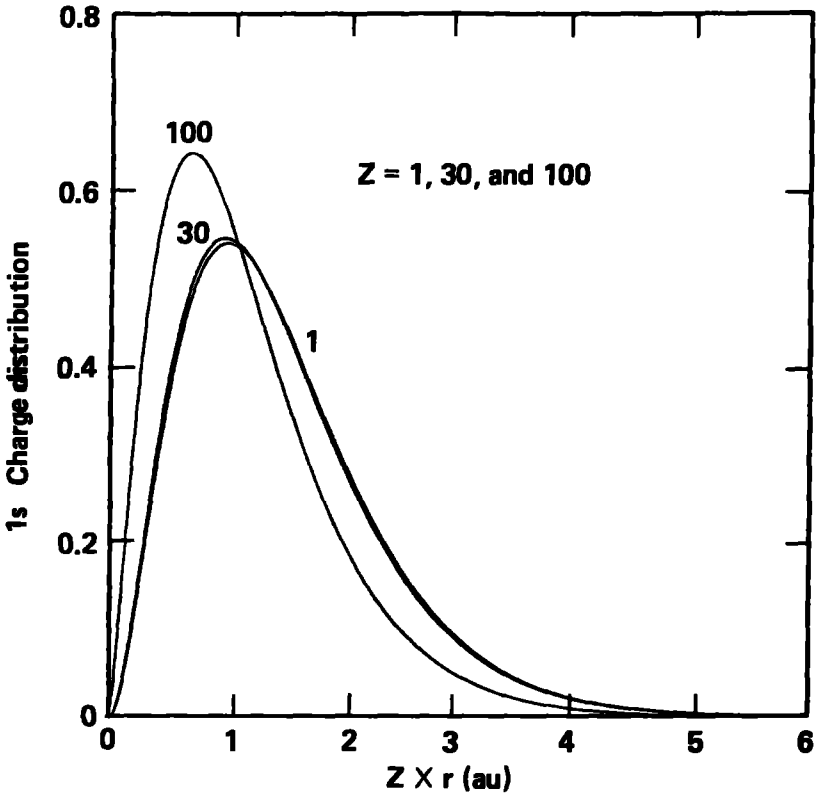

FIG. 2.2. Charge distribution for a Dirac 1s state (courtesy of J. Scofield, private communication).

$$\Phi_\Gamma (1, 2, 3, \ldots, N) = \psi_{\gamma_1} (1)\, \psi_{\gamma_2} (2) \ldots \psi_{\gamma_N} (N) \ . \tag{2.37}$$

In fact, this would be the true form of Φ if the atomic Hamiltonian were just a sum of 1–electron terms,* viz (in atomic units)

$$H \rightarrow H^{(1)} = \sum_{i=1}^{N} H(i) = \sum_{i=1}^{N} \left[-\frac{1}{2} \nabla_i^2 - \frac{Z}{r_i} \right] , \tag{2.38}$$

and did not include the electrostatic interactions among all pairs of electrons,

$$H^{(2)} = \sum_{j>i}^{N} \frac{1}{r_{ij}} \ . \tag{2.39}$$

* For the time being, we ignore fine–structure effects and symmetry requirements. These complicate the mathematics but do not alter the arguments we want to develop.

The purpose of the central-field approximation is to retain the form (2.37), by assuming that each electron can be treated as moving in some averaged effective field of all other electrons.

D. R. Hartree proposed a self-consistent field (SCF) scheme, wherein the effective potential for the i^{th} electron is

$$V(\vec{r_i}) = -\frac{Z}{r_i} + \sum_{j \neq i} \int d\vec{r_i}\, \psi^*(\vec{r_i}) \frac{1}{r_{ij}} \psi(\vec{r_j}) \ . \tag{2.40}$$

The basic idea is easily visualized by the flowchart which follows. The justification of this scheme follows from a variational calculation in which the energy $\langle \Phi | H | \Phi \rangle$ is minimized, subject to the N constraints that each orbital remains normalized; it turns out that the Lagrange multipliers ε_i are the 1-electron orbital energies.

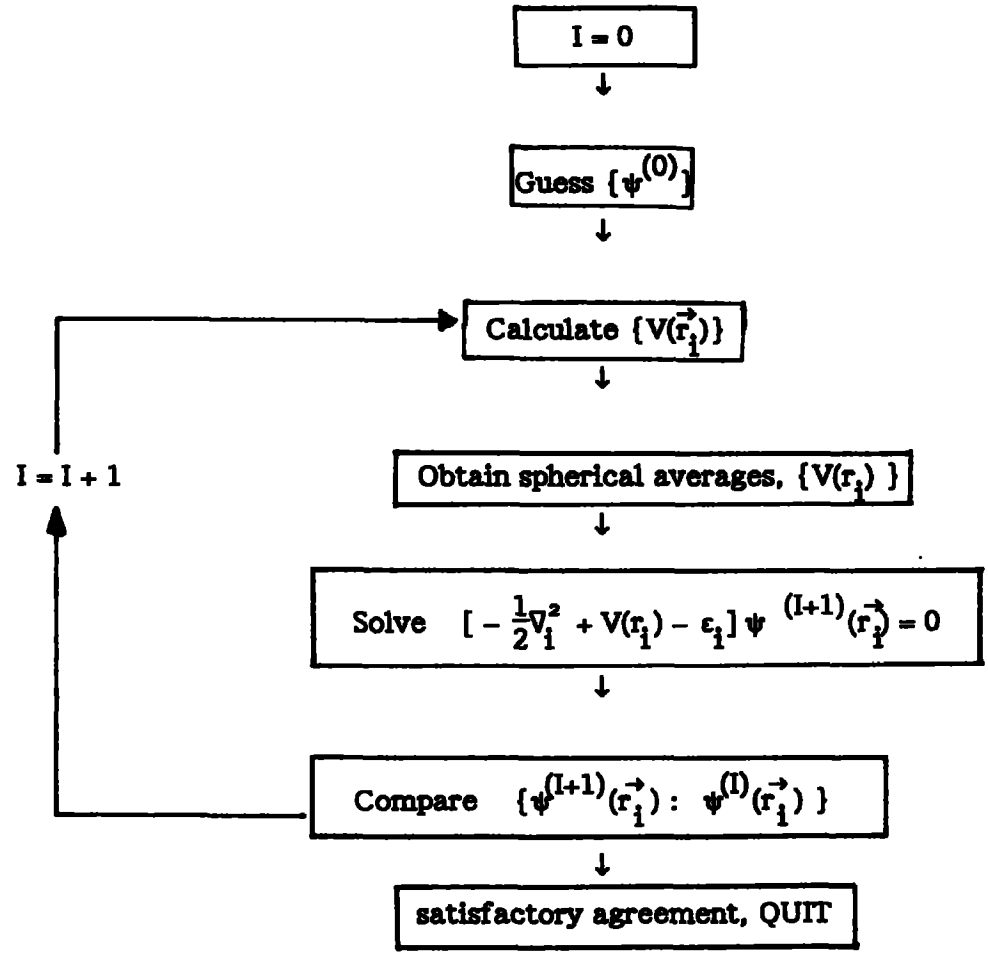

N–Electron Wavefunction; Configurations

The central field approximation is basic to nearly all atomic structure calculations, and so we now devote some time to discussing the product wave function Φ_Γ of Eq. (2.37). This discussion will lead us into the abyss of angular momentum coupling, but first we need to establish some important symmetry results.

By definition, elementary particles of a given kind are indistinguishable from one another. Thus, the Hamiltonian of an N–particle system is not affected by any re–labelling we might choose to do of these particles,

$$H(1, 2, 3, \ldots, N) = H(2, 3, 1, \ldots, N) = \text{etc.}$$

This can be formalized by defining permutation operators Π for which we can write

$$(\Pi, H) = 0 \ . \tag{2.41}$$

(In this case above Π had the effect of exchanging 1 and 2, and then 1 and 3.) For an N–particle system, there are N! possible permutations "p", each of which generates a particular wavefunction $\Pi_p \Phi_\Gamma$. Some of the N ! wavefunctions so formed will be linear combinations of others, but many will be linearly independent – this is the manifestation of exchange degeneracy.

It is an observed fact of nature that only certain wavefunctions are actually realized, and that all physical wavefunctions have a particularly simple property with respect to two–particle interchange, $\Pi(i \leftrightarrow j)$,

$$\Pi(i \leftrightarrow j)\Phi_\Gamma = \begin{cases} +\Phi_\Gamma\text{: symmetrical state.} \\ -\Phi_\Gamma\text{: antisymmetrical state.} \end{cases} \tag{2.42}$$

All many–electron wavefunctions require the (–) sign. A convenient way of contructing products Φ with the correct symmetry is by means of Slater determinants. If, for example, we have a 3–electron system, in which the electrons occupy quantum states a, b, and c, we write

$$\Phi_{abc}(1, 2, 3) = \frac{1}{\sqrt{3!}} \begin{vmatrix} \psi_a(1) & \psi_b(1) & \psi_c(1) \\ \psi_a(2) & \psi_b(2) & \psi_c(2) \\ \psi_a(3) & \psi_b(3) & \psi_c(3) \end{vmatrix} \tag{2.43}$$

The factor $(N!)^{-1/2}$ is for normalization. An interchange of particles corresponds to an interchange of rows, which changes the sign of the determinant. In this form, the Pauli exclusion principle is transparent:

No two electrons in a given system can occupy the same quantum state.

As we noted above, if the electron–electron interaction energy, Eq. (2.39) were negligible, then a product wavefunction of the form (2.37) would be a correct representation of the atom. And, in this simple case, the complete specification of the quantum state Γ would be the orbital configuration, the listing of (n,ℓ)–values of all the different electrons. For instance, the ground–state configuration of uranium is

$$(1s)^2\ (2s)^2\ (2p)^6\ (3s)^2\ (3p)^6\ (3d)^{10}\ (4s)^2\ (4p)^6\ (4d)^{10}\ (4f)^{14}$$

$$(5s)^2\ (5p)^6\ (5d)^{10}\ (5f)^3\ (6s)^2\ (6p)^6\ (6d)\ (7s)^2$$

The exponents indicate the number of equivalent electrons, i.e., those with the same $(n\ell)$–values; and the standard spectroscopic notation has been used:

ℓ	0	1	2	3	4	5	.	.	.
designation	s	p	d	f	g	h	.	.	.

Because of the Pauli exclusion principle, the maximum number of electrons in an atom that can have the same values of (n,ℓ) is $2(2\ell+1)$. A given (n,ℓ) pair is called a subshell.

Unfortunately, a Hamiltonian like Eq. (2.38) is accurate only in the limit $Z >> N$. The real world is more complicated, much more complicated: there are many more states in atoms than can be generated just by changing electron orbitals. How do we go about describing these states? A basic postulate of quantum mechanics tells us that, for any quantized system (= atom), there is a maximal number of physical quantities that can be measured simultaneously. The actual number depends on the system being observed. All of the operators corresponding to these observables must commute with one another. Thus, if there are ν such operators $\{\Lambda_\nu\}$ for a given problem, and their eigenvalues are λ_1, λ_2, etc., then in Dirac's ket notation a quantum state of the system is

$$|\Gamma> = |\lambda_1, \lambda_2, \ldots, \lambda_\nu> . \qquad (2.44)$$

We definitely want to characterize each atomic state by its energy, so we seek operators that commute with H. How many do we need? The answer is that, in addition to specifying the configuration, we need 2N, where N is a sum over unfilled subshells of the following quantity $\tilde{n}$:

if number of subshell e^- is $p \leq 2\ell + 1$, $\quad \tilde{n} = p$

if number of subshell e^- is $p \geq 2\ell + 1$, $\quad \tilde{n} = 2(2\ell+1) - p$

For example, the ground state of uranium requires 2(3+1) = 8 quantum numbers, because of the unfilled $(5f)^3$ (6d) subshells.

Most early work in spectroscopy dealt with the light elements ($Z_{nuc} < 26$), for which at worst there usually is an open (2p) or (3p) subshell. Therefore, the most quantum numbers needed then was $2(2\ell + 1) = 6$. In 1925, Russell and Saunders showed that the main features of complex spectra could be understood when the atomic states are characterized by the composite orbital and spin angular momenta,

$$\vec{L} = \sum_{i=1}^{N} \vec{\ell}_i \quad \text{and} \quad \vec{S} = \sum_{i=1}^{N} \vec{s}_i \ , \tag{2.45}$$

both of which can be shown to commute with the central field Hamiltonian. Fine-structure effects require one also to specify the atom's total angular momentum

$$\vec{J} = \vec{L} + \vec{S} \ ; \tag{2.46}$$

and, if the atom is subjected to an external electromagnetic field, one must in addition specify the eigenvalue of J_Z, commonly denoted M. Thus, in the Russell–Saunders scheme, we write for Eq. (2.44)

$$| \Gamma > \ = \ | \text{ configuration specification; LSJM} > \ . \tag{2.47}$$

(The remaining quantum numbers are intermediate (LS) and "seniority" numbers, which were introduced by Racah in the 1940's.)

The standard spectroscopic notation is:

$^{2S+1}L_J$, with

L	0	1	2	. . .
designation	S	P	D	. . .

The following nomenclature is encountered frequently in connection with state designations.

MULTIPLICITY: $(2S + 1) = \begin{cases} \text{singlet, } S = 0 \\ \text{doublet, } S = 1/2 \\ \text{triplet, } S = 1 \end{cases}$

TERM: ^{2S+1}L

LEVEL: $^{2S+1}L_J$

Why does the Russell–Saunders scheme work so well for light elements? The answer lies partly in the "goodness" of the central field approximation, and partly in the interactions not included in that picture. Specifically, these missing parts, and their relative mangitudes are

$$\begin{pmatrix}\text{Exchange interactions} \\ \text{due to } \Phi \text{ antisymmetry}\end{pmatrix} > \begin{pmatrix}\text{non–spherical} \\ \text{part of } V(\vec{r})\end{pmatrix} > \begin{pmatrix}\text{fine–structure} \\ \text{interactions}\end{pmatrix} \qquad (2.48)$$

The angular momenta S, L, J, in some sense characterize these effects, respectively. Figure 2.3 illustrates the break–up of a configuration into levels.

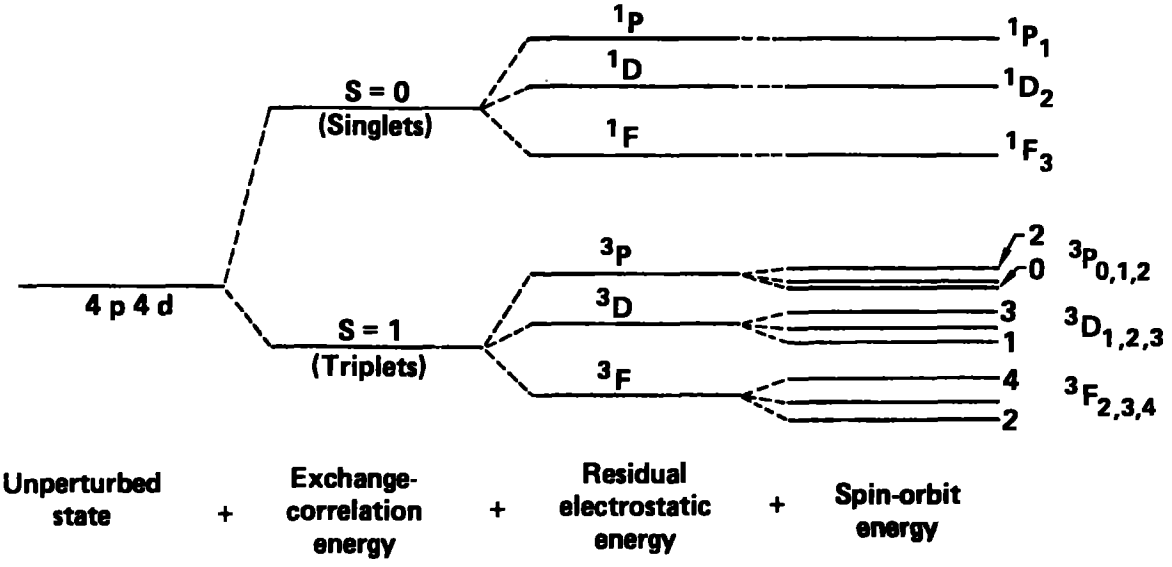

FIG. 2.3. The development of level structure in L–S coupling.

Coupling of Angular Momenta

So far, you have heard good news – the LSJ representation works well for light elements. Now for some bad news.

Bad News Item #1: In defining L, S, and J, I did not tell you how the angular momenta are to be added. You remember "vector addition" from your introductory quantum class so that $\vec{L}_{12} = \vec{\ell}_1 + \vec{\ell}_2$ ranges in magnitude from $|\vec{\ell}_1 - \vec{\ell}_2|$ to $|\vec{\ell}_1 + \vec{\ell}_2|$, in integral steps. Of course, it is trivial to extend this, one $\vec{\ell}$–value at a time. But, what if I choose one scheme, and you another:

$$\text{ME: } (\vec{\ell}_1 + \vec{\ell}_2) + \vec{\ell}_3 = \vec{L}_{123} \qquad \text{YOU: } \vec{\ell}_1 + (\vec{\ell}_2 + \vec{\ell}_3) = \vec{L}_{123} \ .$$

Even if we have the same $\vec{L}_{123}$ values, our product wavefunctions will not be identical! They will, however, be related by a unitary transformation, which can be thought of as an angular momentum re–coupling.

The addition of and recoupling of angular momenta is beautifully handled by Racah's methods, which give rise to the 3^n–j symbols, such as

$$\begin{pmatrix} \ell_1 & \ell_2 & \ell_{12} \\ m_1 & m_2 & m_{12} \end{pmatrix} \quad , \quad \begin{Bmatrix} \ell_1 & \ell_2 & \ell_3 \\ s_1 & s_2 & s_2 \end{Bmatrix} \quad , \quad \begin{Bmatrix} \ell_1 & \ell_2 & \ell_{12} \\ s_1 & s_2 & s_{12} \\ j_1 & j_2 & j_{12} \end{Bmatrix} \quad , \text{ etc.}$$

Modern atomic physics literature is replete with these quantities. We cannot delve into their properties in these lectures, but when you encounter them, mentally replace them by some number whose magnitude is less than 1. If necessary, actual values can be gotten from extensive tables, such as M. Rotenberg, et al., (1959) "The 3–j and 6–j Symbols."

Bad News Item #2. When Z is large, say $Z \geq 30$, the LSJ scheme fails. That is because the ordering of effects is no longer that given by Eq. (2.48). The first two terms scale approximately as Z, but the fine–structure interaction scales as Z^4 and eventually overtakes the others. When this happens, $\vec{\ell}_i$ and $\vec{s}_i$ of an individual electron interact strongly, and one needs to adopt what is called jj coupling:

$$\vec{j}_i = \vec{\ell}_i + \vec{s}_i; \quad \vec{J} = \sum_{i=1}^{N} \vec{j}_i \ . \tag{2.49}$$

In jj coupling the orbitals are

$$s_{1/2},\ p_{1/2},\ p_{3/2},\ d_{3/2},\ d_{5/2},\ f_{5/2},\ \ldots, \tag{2.50}$$

and in an atom, no more than 2j+1 electrons can have the same (nℓj)–values.

In principle, all necessary re–coupling can be accomplished via Racah methods, but in practice this gets very complicated. What's worse, in a large number of interesting systems the true coupling is "intermediate" to LS and jj, since all three terms in Eq. (2.48) are comparable. One example, for the p^2 configuration, is shown below, where level energies are plotted as a function of χ ~ (spin–orbit interaction) ÷ (electrostatic interaction). The notation on the right hand side of the figure is $(j_1\ j_2)^J{}_{12}$.

Bad News Item #3. Yet another complication is tht energetically adjacent states belonging to different configurations can interact with each other, which then requires the wavefunctions of these configuration–mixed states to be represented as linear combinations of single–configuration states such as Eq. (2.47).

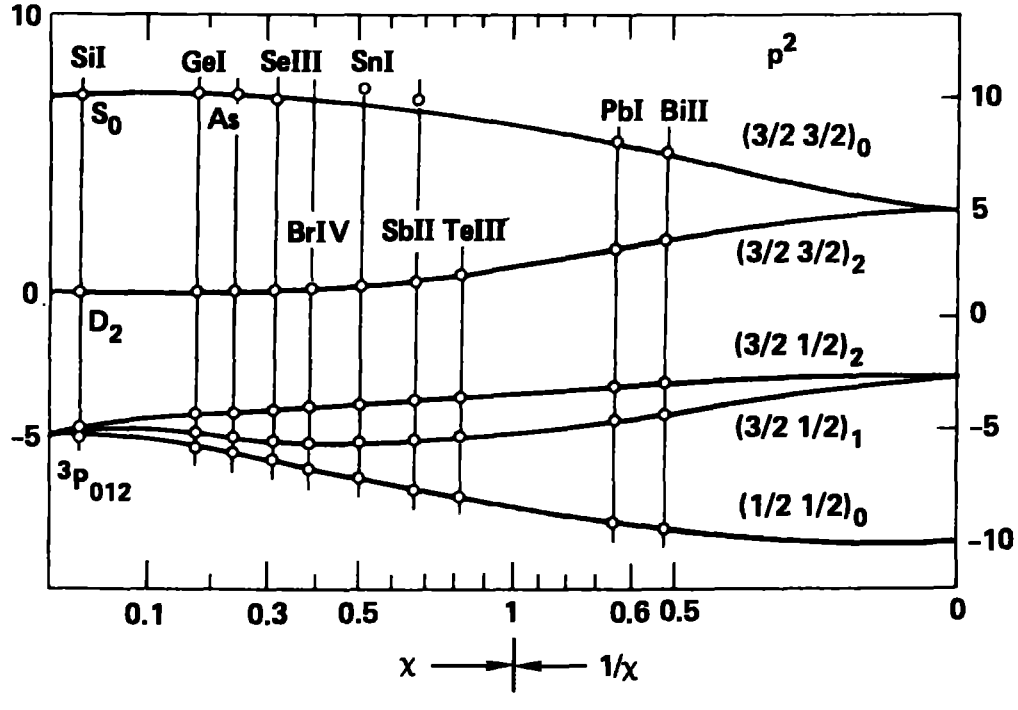

FIG. 2.4. Transition from LS coupling to jj coupling for the configuration p^2.

Relativistic Many–Electron Atom (a précis)

G. Breit* generalized the Dirac Equation to the two–electron atom. His relativistic Hamiltonian is

$$H(1,2) = H_D(1) + H_D(2) + \frac{e^2}{r_{12}}\left[1 - \frac{1}{2}\,\alpha_1 \cdot \alpha_2 - \frac{(\alpha_1 \cdot \vec{r}_{12})(\alpha_2 \cdot \vec{r}_{12})}{2r_{12}^2}\right] \qquad (2.51)$$

In this equation α_1 and α_2 have the same form given by Eq. (2.18), but operate, respectively, only on electron 1 and 2; H_D is the 1–electron Dirac Hamiltonian of Eq. (2.26). The correction to the term e^2/r_{12} is called the Breit interaction. Although this Hamiltonian is not fully Lorentz invariant (the Breit interaction itself is only approximate), it is the starting point for many N–electron systems.

To obtain a tractable Hamiltonian, good for modest ($Z\alpha$), Bethe and Salpeter carried out what is equivalent to the Pauli approximation and obtained a Hamiltonian for the large component. In addition to the 1–electron Pauli terms, in Eqs. (2.30) and (2.33), their derivation produced terms representing:

1. retardation of $1/r_{12}$ interaction;
2. interaction of $\vec{s}_1$ and $\vec{s}_2$;
3. interaction of $\vec{s}_1$ and $\vec{\ell}_2$; and $\vec{s}_2$ and $\vec{\ell}_1$ (spin–other orbit);
4. spin–orbit interactions $\propto \vec{s}_1 \cdot \vec{\ell}_1$ and $\vec{s}_2 \cdot \vec{\ell}_2$, but which involve the electric field of the other electron, instead of the nuclear electric field.

All of these terms, plus any radiative corrections, are invariably treated as perturbations (see, especially, Drake, (1982), "Advances in Atomic and Molecular Physics," Vol. 18). At best the structure of heavy systems is computed using a central field approximation, but with the one–electron orbitals being solutions of a Dirac equation with a non–Coulombic V(r).

The current computational status of things is summarized in Table 2.2.

The Nucleus

As a last point, we mention that all our discussion so far has assumed the nucleus to be a point charge with infinite mass and no angular momentum. The fact is that all of

*Phys. Rev. 34, 533 (1929); 36, 383 (1930); 39, 616 (1932).

these assumptions are, in general, wrong. This is revealed in small but interesting perturbations of electronic states. Again, we are forced in Table 2.3 merely to summarize these effects; elaborations are to be found in the texts we cited at the beginning of these lectures.

TABLE 2.2. Central Field Calculations.

Name	Hamiltonian	Wavefunction	Well-documented Computer codes
Hartree	non-relativistic no exchange interactions no fine-structure	product of 1-electron orbitals	many
Hartree-Fock	non-relativistic no fine-structure	Slater determinant (1 or more)	C. Froese-Fisher
Hartree-Fock-Slater	non-relativistic approximate exchange interaction no fine-structure	Slater determinant (1 or more)	J. Desclaux
Dirac-Fock	relativistic	Slater determinant (1 or more)	J. Desclaux I. Grant
Dirac-Fock-Slater	relativistic approximate exchange interaction	Slater determinant (1 or more)	————

TABLE 2.3. Nuclear Effects in Atomic Structure.

- Finite mass changes reduced mass, causes isotope shifts
- Finite size causes departure of $\phi(r)$ from pure Coulomb inside nucleus; level shifts depend on nuclear shape and volume.
- Angular momentum causes hyperfine splitting of atomic levels,

$$\vec{F}_{atom} = \vec{I}_{nucleus} + \vec{J}_{electrons}$$

LECTURE #3 – RADIATIVE AND COLLISIONAL TRANSITIONS

In the preceding lecture, we discussed the eigenvalue problem for atomic systems. From this point on, we assume that solutions of the SE,

$$[H(\text{atom}) - E_\Gamma]\,\psi_\Gamma = 0 \ , \tag{3.1}$$

are available at some level of approximation. In this lecture, we consider the problem of transitions between atomic states caused by interactions with radiation or other particles. Frequently, such problems are treated within the context of perturbation theory.

Resumé of Perturbation Theory

Dirac's "variation of the constants" method gives the amplitude $a_{\Gamma'\Gamma}(t)$ for the atomic transition $\Gamma \to \Gamma'$, due to the action of a time–dependent perturbation V(t):

$$a_{\Gamma'\Gamma}(t) = -\frac{i}{\hbar} \int_{-\infty}^{t} V_{\Gamma'\Gamma}(t)\, e^{i\omega_{\Gamma'\Gamma} t}\, dt \ , \tag{3.2}$$

where

$$V_{\Gamma'\Gamma} = \langle \Gamma' | V(t) | \Gamma \rangle \ , \text{ and } \hbar\omega_{\Gamma'\Gamma} = E_{\Gamma'} - E_\Gamma \tag{3.3}$$

are the transition matrix element and the transition energy, respectively.

One class of problems is represented by perturbations that turn on and then turn off, and vanish in the limits $t \to \pm\infty$. Let's use a Gaussian form to represent them,

$$V(t) = \tilde{V}\,(2\pi)^{-1/2} \exp\left[-(t-t_o)^2/2\tau^2 \right] \ . \tag{3.4}$$

Substitution into Eq. (3.2) yields the transition probability,

$$P_{\Gamma'\Gamma} = |\, a_{\Gamma'\Gamma}(t \to +\infty)\,|^2 \Rightarrow |\, \tilde{V}_{\Gamma'\Gamma}\, \tau/\hbar\,|^2 \exp\left[-(\omega_{\Gamma'\Gamma}\, \tau)^2 \right] \ . \tag{3.5}$$

A perturbation is sudden if $\omega_{\Gamma'\Gamma}\tau \ll 1$, and adiabatic if $\omega_{\Gamma'\Gamma}\tau \gg 1$. Note that $P_{\Gamma'\Gamma}$ has its maximum value when $\omega_{\Gamma'\Gamma}\tau = 1$.

Another class of problems deals with periodic perturbations, viz.

$$V(t) = \tilde{V} \cos \omega t \ , \tag{3.6}$$

which persist indefinitely. In such cases, one calculates a transition probability per unit time,

$$\frac{d}{dt} P_{\Gamma'\Gamma}(t) = \frac{2\pi}{\hbar^2} |\tilde{V}_{\Gamma'\Gamma}|^2 \delta(\omega_{\Gamma'\Gamma} - \omega) \ . \tag{3.7}$$

An important special case of periodic perturbations is obtained in the limit $\omega \to 0$: V is independent of time, except for its being turned "on" and then "off". Here again, one computes a transition probability per unit time, with the result that [in Eq. (3.7)] the delta function $\delta(\omega_{\Gamma\Gamma'} - \omega)$ is replaced by $\delta(\omega_{\Gamma\Gamma'})$.

Finally, suppose that Γ is one of several degenerate states, whose density (i.e., number of states per unit energy interval), is $\rho(E_\Gamma)$; for instance, a plane wave of momentum $\vec{p} = \hbar\vec{k} = m\vec{v}$ has a density of states

$$\rho(E) = \frac{4\pi p^2 dp}{(2\pi\hbar)^3 dE} \ . \tag{3.8}$$

It is intuitively obvious that the transition probability should be proportional to $\rho(E)$. In particular, for the constant perturbation we have, altogether,

$$W_{\Gamma'\Gamma} = \frac{d}{dt} |a_{\Gamma'\Gamma}(t)|^2 = \frac{2\pi}{\hbar} |\tilde{V}_{\Gamma'\Gamma}|^2 \rho(E_{\Gamma'}) \ . \tag{3.9}$$

This very important formula is called "Fermi's Golden Rule."

Cross Sections and Detailed Balance

Consider the apparatus shown in the figure below. A flux $N_o\vec{v}_o$ of particles is incident on a scattering center, or target. A detector is placed a considerable distance away, and at an angle θ with respect to $\vec{v}_o$. The differential cross section for the scattering of incident particles into the detector, plus causing the transition $\Gamma \to \Gamma'$ within the target, is defined as

$$I_{\Gamma'\Gamma}(\theta, v_o) \equiv \frac{\text{\# detections/time/solid angle}}{N_o v_o} \tag{3.10}$$

Integration over solid angles $d\Omega$ yields the total scattering cross section,

$$Q_{\Gamma'\Gamma}(v_o) = \int\int I_{\Gamma'\Gamma}(\theta, v_o)\, d\Omega \ . \tag{3.11}$$

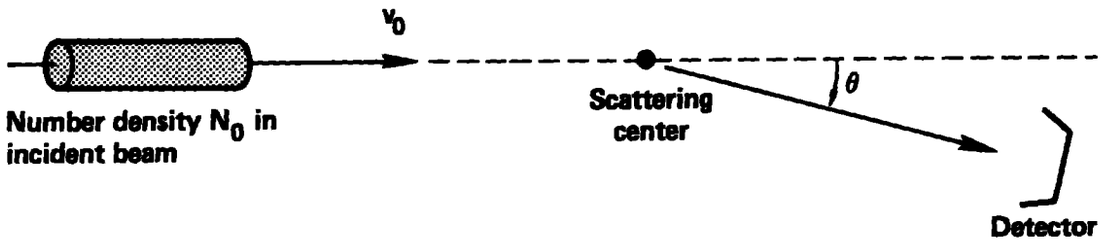

FIG. 3.1. Idealized scattering experiment.

Suppose we choose to treat a collision as a time-dependent perturbation problem. Let b be the impact parameter for a particular collision trajectory, i.e., it would be the distance of closest approach of the target and the incident particle, if their relative motion were rectilinear. We can use Newtonian equations of motion to compute V(t) and, with it, a probability $P_{\Gamma'\Gamma}(b, v_o)$ for the transition (classically, b and θ are uniquely related). From it we determine the total cross section,

$$Q_{\Gamma'\Gamma}(v_o) = 2\pi \int P_{\Gamma'\Gamma}(b, v_o)\, b\, d\, b \ . \tag{3.12}$$

This is the basis of the impact parameter method.

Alternatively, we can choose to treat a collision as an eigenvalue problem; we then solve

$$[H(\text{target}) + H(\text{projectile}) + V - E_{\text{total}}]\, \Psi_{\text{total}} = 0 \ , \tag{3.13}$$

with V being a function of relative positions, spins, etc., but <u>not</u> a function of time. The flux in this case is just $\vec{v}_o$, and the differential cross section is

$$Q_{\Gamma'\Gamma}(v_o) = \frac{1}{v_o} \left[\frac{dP_{\Gamma'\Gamma}(t)}{dt}\right] , \tag{3.14}$$

where dP/dt is gotten from "Fermi's Golden Rule."

In general, there is a degeneracy $g_{\Gamma'}$ of the target's final states, in addition to the degeneracy $\rho(E_{\Gamma'}) \propto v_f$, the speed of the scattered particle. Thus, we have

$$Q_{\Gamma'\Gamma}(v_o) = \frac{2\pi}{\hbar} |\langle \Gamma' | \tilde{V} | \Gamma \rangle|^2 \left[\frac{4\pi\mu^2 \, g_{\Gamma'} \, v_f}{(2\pi\hbar)^3 v_o}\right] , \tag{3.15}$$

where μ is the reduced mass.

Finally, consider the reverse process, wherein the incident particle, with velocity $\vec{v}_f$ scatters from the target and causes the transition $\Gamma' \rightarrow \Gamma$. The same arguments that got us Eq. (3.15) can also be used to obtain the cross section for this back reaction. Because only the square of the absolute value of $V_{\Gamma'\Gamma}$ appears in both formulae, we find that

$$v_o^2 \, g_\Gamma \, Q_{\Gamma' \leftarrow \Gamma}(v_o) = v_f^2 \, g_{\Gamma'} \, Q_{\Gamma \leftarrow \Gamma'}(v_f) \tag{3.16}$$

This is the "Principle of Detailed Balance," which will prove to be very useful.

In the remainder of this lecture, we apply these ideas to transitions between bound states of an ion. Ionization and recombination processes will be treated in the last lecture.

The Radiation Field, Classical and Quantized

The standard classical treatment of the electromagnetic field is in terms of scalar and vector potentials. When no sources are present, the scalar potential $\phi=0$, and the Coulomb gauge is usually chosen: $\vec{\nabla} \cdot \vec{A} = 0$. A useful description of the vector potential is its Fourier decomposition in three dimensions, with the imposed boundary condition that $\vec{A}$ be periodic in a box of dimension $L \gg$ atomic dimensions. Thus,

$$\vec{A}(\vec{r}, t) = \sum_{q=1}^{2} \hat{\varepsilon}_q \sum_{\vec{k}} \{ A_{\vec{k},q} \exp[i(\vec{k} \cdot \vec{r} - \omega t)] + \text{c.c.} \} \, , \tag{3.17}$$

where $\hat{\varepsilon}_1$ and $\hat{\varepsilon}_2$ are unit vectors representing the different axes of polarization, $\omega=ck$ is the angular frequency, $\vec{k}$ is the propagation vector, and c.c. denotes the complex conjugate of the preceding term. In terms of the wave amplitudes $A_{\vec{k}q}$ and $A^*_{\vec{k}q}$, the energy density of the radiation field is

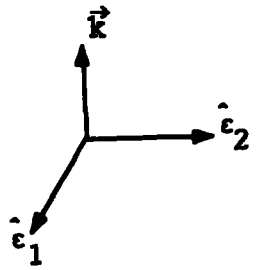

$$U = \frac{1}{2\pi} \sum_{\vec{k},q} k^2 \, | A_{\vec{k},q} |^2 \, . \tag{3.18}$$

The quantized electromagnetic field requires, for its description, the number of photons $N_{\vec{k},q}$ having specific polarization and momentum $\hbar\vec{k}$. Thus, we write,

$$|\text{EM field}\rangle = |N_{\vec{k}_1\epsilon_1}\rangle\ |N_{\vec{k}_1\epsilon_2}\rangle\ |N_{\vec{k}_2\epsilon_1}\rangle \ldots \quad . \tag{3.19}$$

The simple product representation is possible because each mode $(\vec{k},q)$ is treated as an independent harmonic oscillator. When canonical variables are constructed from $\vec{A}$ and $\vec{A}^*$, we can effect the transition to a quantized field by making replacements in Eq. (3.17),

$$A_{\vec{k},q} \rightarrow \left(\frac{2\pi\hbar c^2}{\omega V}\right)^{1/2} a_{\vec{k},q} \quad , \quad A^*_{\vec{k},q} \rightarrow \left(\frac{2\pi\hbar c^2}{\omega V}\right)^{1/2} a^\dagger_{\vec{k},q} \quad . \tag{3.20}$$

The most important properties of the operators a and $a^\dagger$ are

$$a_{\vec{k},q}\ |\ N_{\vec{k},q}\rangle = \sqrt{N_{\vec{k},q}}\ |\ N_{\vec{k},q} - 1\ \rangle \ ,$$

$$a^\dagger_{\vec{k},q}\ |\ N_{\vec{k},q}\rangle = \sqrt{N_{\vec{k},q} + 1}\ |\ N_{\vec{k},q} + 1\ \rangle \ ,$$

$$a^\dagger_{\vec{k},q}\ a_{\vec{k},q}\ |\ N_{\vec{k},q}\ \rangle = N_{\vec{k},q}\ |\ N_{\vec{k},q}\ \rangle \quad . \tag{3.21}$$

Given these properties, it is evident why a, $a^\dagger$ and $a^\dagger a$ are called the destruction, creation, and number operators, respectively.

Interaction of Matter and Radiation*

The interaction is treated as a perturbation, and the correct form of the non-relativistic Hamiltonian is gotten from Pauli's approximation. For each atomic electron, there are three terms involving $\vec{A}$:

$$V(r_i) = \alpha\vec{A} \cdot \vec{p}_i + \frac{1}{2}\,\alpha^2\vec{A} \cdot \vec{A} + \alpha\vec{s}_i \cdot (\vec{\nabla} \times \vec{A}) \quad . \tag{3.22}$$

(Atomic units have been used.) The first term represents electric multipole interactions. The last of these three terms represents magnetic multipole interactions; it is ignorable if the first term can cause radiative transitions, because the curl operator has the effect of introducing another factor of α. The middle term, also smaller by a factor of α, contains

*In addition to texts cited in the first lecture, see especially the recent review by Heffernan and Liboff (1982), JQSRT 27, pp. 55–77.

products of the operators a and $a^\dagger$. It is responsible for Rayleigh (elastic) scattering and Raman (inelastic) scattering.

Suppose we are interested in a transition in which an atom starts in state Γ, emits or absorbs a single photon $(\vec{k},q)$, and ends in state Γ'. The only part of the radiation field's initial wavefunction that is involved is the ket $|N_{\vec{k}q}>$, and the transition matrix element reduces to a single term,

$$\left\{ \begin{matrix} \text{emission} \\ \text{absorption} \end{matrix} \right\} \rightarrow \langle\, N_{\vec{k},q} \pm 1\ ;\ \Gamma' \,|\, V \,|\, N_{\vec{k},q}\ ;\ \Gamma \rangle$$

$$= \left(\frac{2\pi\alpha}{kL^3}\right)^{1/2} \begin{bmatrix} \sqrt{N_{\vec{k},q}+1} \\ \sqrt{N_{\vec{k},q}} \end{bmatrix} e^{\pm i\omega t} \langle\, \Gamma' \,|\, \hat{\epsilon}_q \cdot \sum_{i=1}^{N} \vec{p}_i e^{\mp i \vec{k}\cdot\vec{r}_i} \,|\, \Gamma \rangle \ . \qquad (3.23)$$

At this point, we invoke Fermi's Golden Rule to compute the transition probability per unit time. The additional information needed is the number of modes, per unit energy interval, for a photon propagating into the solid angle $d\Omega$ about $\vec{k}$, and in the wave vector interval $(\vec{k},\ \vec{k}+d\vec{k})$:

$$d\rho(\vec{k}) = \frac{\alpha L^3 k^2}{(2\pi)^3} d\Omega \ . \qquad (3.24)$$

Of course, k must be such that energy is conserved, i.e., $|E_\Gamma - E_{\Gamma'}| = \omega = k/\alpha$ (in at. units).

Altogether then,

$$\frac{dW_{\Gamma'\Gamma}}{d\Omega} = \left(\frac{\alpha^2 k}{2\pi}\right) \left| \langle \Gamma' \,|\, \hat{e}_q \cdot \sum_{i=1}^{N} \vec{p}_i e^{\mp i \vec{k}\cdot\vec{r}_i} \,|\, \Gamma \rangle \right|^2 \cdot \begin{bmatrix} N_{\vec{k},q}+1 \\ N_{\vec{k},q} \end{bmatrix} \qquad (3.25)$$

In this, our fundamental result, upper values correspond to emission, and lower values to absorption. Especially important is the stimulated emission factor proportional to $N_{\vec{k},q}$, which is responsible for lasing phenomena.

The dipole approximation (i.e., an E1 transition) is obtained by putting

$$e^{\pm i \vec{k}\cdot\vec{r}_i} \rightarrow 1 \pm i\vec{k}\cdot\vec{r}_i \ . \qquad (3.26)$$

Since, for a bound electron, r typically is of the order $n^2 a_o/Z$, this simplification is adequate as long as the photon energy is not too large, $E_k = \hbar ck \leq (Z/n^2)$ keV. After Eq. (3.26), the next step in the dipole approximation involves the operator identity

$$\vec{p}_i = \frac{i}{\hbar} [H(\text{atom}), \vec{r}_i] \tag{3.27}$$

and the definition of the atomic dipole moment, $\vec{D} = -e \Sigma \vec{r}_i$. Then, if we assume that the radiation field is isotropic and unpolarized, viz

$$N_{\vec{k},1} = N_{\vec{k},2} = \frac{1}{2} N_\omega , \tag{3.28}$$

we can sum over polarization states and integrate over propagation directions to obtain a transition probability per unit time

$$W_{\Gamma'\Gamma} \begin{bmatrix} \text{E1 emission} \\ \text{E1 absorption} \end{bmatrix} = \frac{4}{3} k^3 \, |\langle \Gamma' | \vec{D} | \Gamma \rangle|^2 \begin{bmatrix} \frac{1}{2} N_\omega + 1 \\ \frac{1}{2} N_\omega \end{bmatrix} \tag{3.29}$$

(In natural units, we replace k^3 by $k^3/\hbar = \omega^3/\hbar c^3$.) Finally, if we use the fact that the specific energy density of radiation is directly proportional to N_ω, namely $U_\omega = (\hbar\omega^3/\pi^2 c^3) \cdot (\frac{1}{2} N_\omega)$, we obtain the familiar Einstein coefficients; reverting to natural units these are

$$W_{\Gamma'\Gamma}(\text{spontaneous emission}, \Gamma \to \Gamma') \equiv A_{\Gamma'\Gamma} = \frac{4\omega^3}{3\hbar c^3} |\langle \Gamma' | \vec{D} | \Gamma \rangle|^2 ,$$

$$W_{\Gamma'\Gamma}(\text{stimulated emission}, \Gamma \to \Gamma') \equiv B_{\Gamma'\Gamma} = \frac{4\pi^2}{3\hbar^2} U_\omega \, |\langle \Gamma' | \vec{D} | \Gamma \rangle|^2 , \tag{3.30}$$

$$W_{\Gamma'\Gamma}(\text{absorption}, \Gamma' \to \Gamma) \equiv B_{\Gamma\Gamma'} = \frac{4\pi^2}{3\hbar^2} U_\omega \, |\langle \Gamma | \vec{D} | \Gamma' \rangle|^2 .$$

These results are easily extended to include degenerate atomic states Γ and/or Γ'. Let γ and γ' denote, respectively, the substates of Γ and Γ'. Following an earlier discussion leading to Eq. (3.16), for any of the probabilities $A_{\Gamma'\Gamma}$, $B_{\Gamma'\Gamma}$, or $B_{\Gamma\Gamma'}$, we have simply

$$W_{\Gamma' \leftarrow \Gamma} = \frac{1}{g_\Gamma} \sum_{\gamma' \gamma} W_{\gamma' \gamma} \quad , \tag{3.31}$$

if there is no substate selection. Thus, we obtain $B_{\Gamma' \Gamma} g_\Gamma = B_{\Gamma \Gamma'} g_{\Gamma'}$.

Two other quantities often are used in discussions of matter–radiation interaction. They are

$$\text{line strength: } S_{\Gamma \Gamma'} = \sum_{\gamma' \gamma} | \langle \Gamma' \gamma' | \vec{D} | \Gamma \gamma \rangle |^2 \tag{3.32}$$

$$\text{absorption oscillator strength: } f_{\Gamma \leftarrow \Gamma'} = \frac{2 m_e \omega}{3 \hbar e^2 g_{\Gamma'}} S_{\Gamma' \Gamma} \quad . \tag{3.33}$$

Electric Dipole (E1) Selection Rules

Restrictions, or selection rules, for radiative transitions arise from the evaluation of the dipole matrix element $\langle \Gamma' | \vec{D} | \Gamma \rangle$. Regardless of the coupling scheme used to describe the atomic states, we find that E1 transitions can only occur if

$$\Delta J = | J_\Gamma - J_{\Gamma'} | = 0, 1 \quad , \tag{3.34}$$

but $(J_\Gamma = 0) \rightarrow (J_{\Gamma'} = 0)$ is not allowed. Additionally, we can ascribe a parity to each N–electron state

$$\Pi_\Gamma = (-1)^{\sum_i \ell_i} \tag{3.35}$$

as well as to the field's electric multipoles,

$$\Pi_{Em} = (-1)^m \quad . \tag{3.36}$$

Then, conservation of parity can be expressed succinctly as

$$\Pi_{\Gamma'} \Pi_{Em} \Pi_\Gamma = +1 \quad . \tag{3.37}$$

There are additional selection rules, that we will present shortly, that apply to particular angular momentum coupling schemes, i.e., LS or jj.

Forbidden Transitions

When a particular transition violates any E1 selection rule, its dipole line strength factor $S_{\Gamma'\Gamma} = 0$ and the transition is termed "forbidden." However, it may not be strictly forbidden: many transtions can occur via higher order terms in the expansion of exp ($i\vec{k} \cdot \vec{r}$), Eq. (3.26). These terms correspond to higher multipoles – electric quadrupole, electric octopole, etc. – of the electric field's interaction with the atom. Each such term brings another factor of α^2 into the transition probability formula. Moreover, if a transtion is dipole–forbidden, we also need to consider the magnetic multipole terms that arise from the interaction

$$\alpha \sum_{i=1}^{N} \vec{s}_i \cdot (\vec{\nabla} \times \vec{A}) \rightarrow \left(\frac{e\hbar}{2m_e c}\right) \vec{B} \cdot \sum_{i=1}^{N} \vec{\sigma}_i \text{ (natural units)} \quad . \tag{3.38}$$

Since $|\vec{B}| \sim (v/c)|\vec{\mathscr{E}}| \sim Z\alpha|\vec{\mathscr{E}}|$, it is apparent that E2 and M1 transitions have matrix elements of comparable magnitude; and similarly for E3 and M2 transitions, etc. [The various magnetic mutipoles also derive from higher order terms in the expansion of $\exp(i\vec{k}\cdot\vec{r})$.]

The following table summarizes the selection rules that apply to E1 and M1 transitions; E1 selection rules are also given. Incidentally, the parity of a magnetic multipole is

$$\Pi_{Mm} = (-1)^{m+1} \quad . \tag{3.39}$$

Z–Scaling of Radiative Transition Rates

To extract Z–scaling properties of the various multipole contributions to the spontaneous transition rate $A(\Gamma' \leftarrow \Gamma)$, we need the general results (cf. Blatt and Weisskopf, Theoretical Nuclear Physics, Ch. 12, 1952)

$$\begin{aligned} A_{Em}(\Gamma' \leftarrow \Gamma) &\propto \Delta E^{2m+1}\, r^{2m} \quad , \\ A_{Mm}(\Gamma' \leftarrow \Gamma) &\propto \Delta E^{2m+1}\, r^{2m-2} \quad . \end{aligned} \tag{3.40}$$

Since, as we noted earlier, $\Delta E \sim Z^2$ and $r \sim Z^{-1}$, we have

$$A_{Em} \sim Z^{2m+2} \text{ and } A_{Mm} \sim Z^{2m+4} \quad . \tag{3.41}$$

This scaling is exact for non-relativistic hydrogen atoms, and is quite accurate for non-relativistic complex atoms.

Now, typical transition energies are $\Delta E \sim (Z\alpha)^2$ at. units, so each successively higher multipole A-value decreases by approximately a factor of $\alpha^4 \sim 10^{-8}$! Recall that for hydrogen, $A_{E1}(1s \leftarrow 2p) \sim 10^8$ sec^{-1}; thus, we can expect M1 and E2 transitions to have probabilities of order 1 sec^{-1}, M2 and E3 transitions to have probabilities of order 10^{-8} sec^{-1}, and so on.

TABLE 3.1. Selection Rules for Allowed and Forbidden Transitions.

Coupling scheme for which the rules apply:		Electric-Dipole	Magnetic-Dipole	Electric-Quadrupole
[L-S and j-j]	1.	$\Delta J = 0, \pm 1$ ($0 \not\leftrightarrow 0$ forbidden)	$\Delta J = 0, \pm 1$ ($0 \not\leftrightarrow 0$ forbidden)	$\Delta J = 0, \pm 1, \pm 2$ ($0 \not\leftrightarrow 0$; $\frac{1}{2} \not\leftrightarrow \frac{1}{2}$, $0 \not\leftrightarrow 1$, all forbidden)
	2.	$\Delta M_J = 0, \pm 1$	$\Delta M_J = 0, \pm 1$	$\Delta M_J = 0, \pm 1, \pm 2$
	3.	Parity change	No parity change	No parity change
[L-S only]	4.	$\Delta \ell = \pm 1$	$\Delta \ell = 0$ $\Delta n = 0$	$\Delta \ell = 0, \pm 2$
	5.	$\Delta S = 0$	$\Delta S = 0$	$\Delta S = 0$
	6.	$\Delta L = 0, \pm 1$ ($0 \not\leftrightarrow 0$ forbidden)	$\Delta L = 0$	$\Delta L = 0, \pm 1, \pm 2$ ($0 \not\leftrightarrow 0$, $0 \not\leftrightarrow 1$ forbidden)

An excellent summary of radiative transtions in the He isoelectronic sequence has been given by Dalgarno (1971), in a symposium honoring D. Menzel (N.B.S. Special Publ. #353). Figure 3.2 and Table 3.2 have been extracted from his review. In connection with the table there are two things to note: (1) the $2^3S_1 - 1^1S_0$ transition occurs only in a fully relativistic formulation of M1, wherein the 1s and 2s radial functions are not orthogonal [c.f. Eq. (2.9)].; (2) the $2^3P_2 - 1^1S_0$ transition mode is M2; for Z>17, this is faster than the E1 transition $2^3P_2 - 2^3S_1$.

The situation is less satisfactory for the Ne–isoelectronic sequence, whose spectrum is much more complicated and whose wave functions obviously are much harder to compute accurately. The configurations of the lowest excited states of these ions are

$(2s)^2\ (2p)^5$ [3s or 3p or 3d] and $(2s)\ (2p)^{-6}$ [3s or 3p or 3d] ;

a partial energy level scheme is shown in Fig. 3.3. One interesting aspect of these energy levels is that the lowest excited state is $(2s^2\ 2p^5\ 3s)^3P_2$, which can decay radiatively only by an M2 transition. As predicted by Eq. (3.41), the M2 transition rate $\sim Z^{10}$.

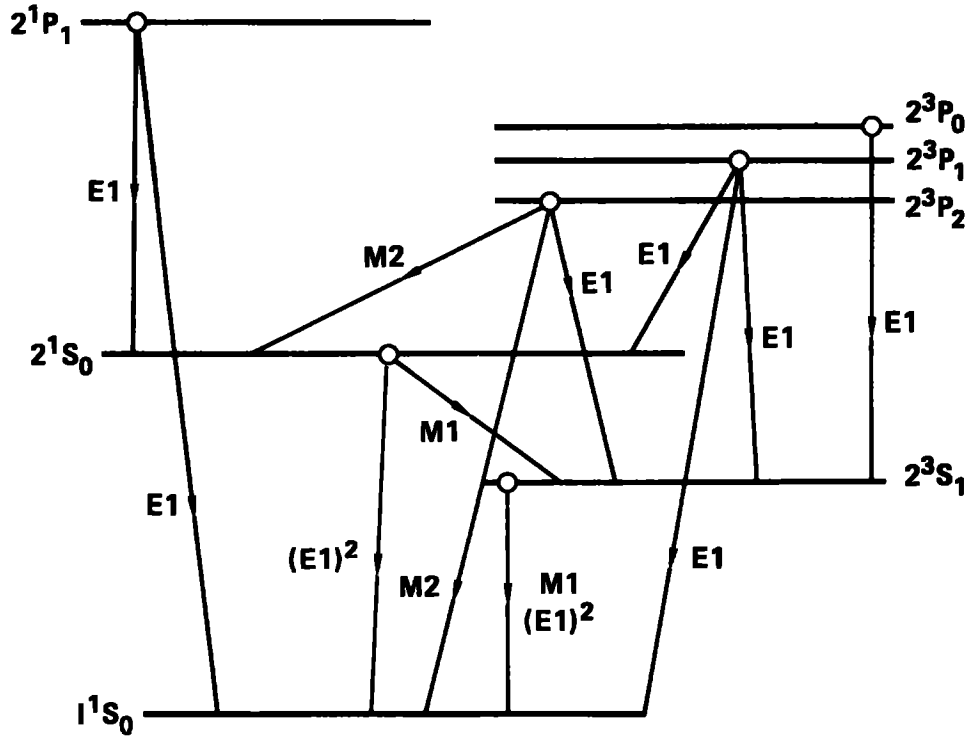

FIG. 3.2. Energy level diagram for neutral helium showing the ordering of the levels.

TABLE 3.2. Radiative Transition Probabilities A for the Helium Sequence (in sec^{-1}).

Z	System	$2^1P_1 - 1^1S_o$*	$2^3P_2 - 1^1S_o$	$2^3S_1 - 1^1S_o$
2	He I	1.80 (9)†	3.27 (–1)	1.27 (–4)
3	Li II	2.56 (10)	3.50 (1)	2.04 (–2)
4	Be III	1.22 (11)	6.17 (2)	5.62 (–1)
5	B IV	3.72 (11)	5.01 (3)	6.70 (0)
6	C V	8.87 (11)	2.62 (4)	4.86 (1)
7	N VI	1.81 (12)	1.03 (5)	2.53 (2)
8	O VII	3.31 (12)	3.34 (5)	1.04 (3)
9	F VIII	5.58 (12)	9.23 (5)	3.61 (3)
10	Ne IX	8.87 (12)	2.27 (6)	1.09 (4)
11	Na X	1.34 (13)	5.10 (6)	2.94 (4)
12	Mg XI	1.96 (13)	1.06 (7)	7.24 (4)
13	Al XII	2.76 (13)	2.09 (7)	1.66 (5)
14	Si XIII	3.78 (13)	3.88 (7)	3.56 (5)
15	P XIV	5.07 (13)	6.91 (7)	7.25 (5)
16	S XV	6.66 (13)	1.18 (8)	1.41 (6)
17	Cl XVI	8.59 (13)	1.96 (8)	2.62 (6)
18	Ar XVII	1.09 (14)	3.14 (8)	4.71 (6)

* From G.W.F. Drake (unpublished).
† 1.80 (9) $\equiv 1.80 \times 10^9$

In Table 3.3 we present some Ne-like ion radiative rates, computed with a Dirac-Fock code by Fielder, Lin, and Ton-That (1979 Phys. Rev. A19, 741). At Z=10 (Ne^o), the lowest J=1 state of the configuration ($p_{3/2}\ s_{1/2}$) is 88% $^3P_1$, but at Z=92, its character is 66% $^1P_1$. Therefore its decay rate to the ground state increases with Z primarily because of this configuration mixing.

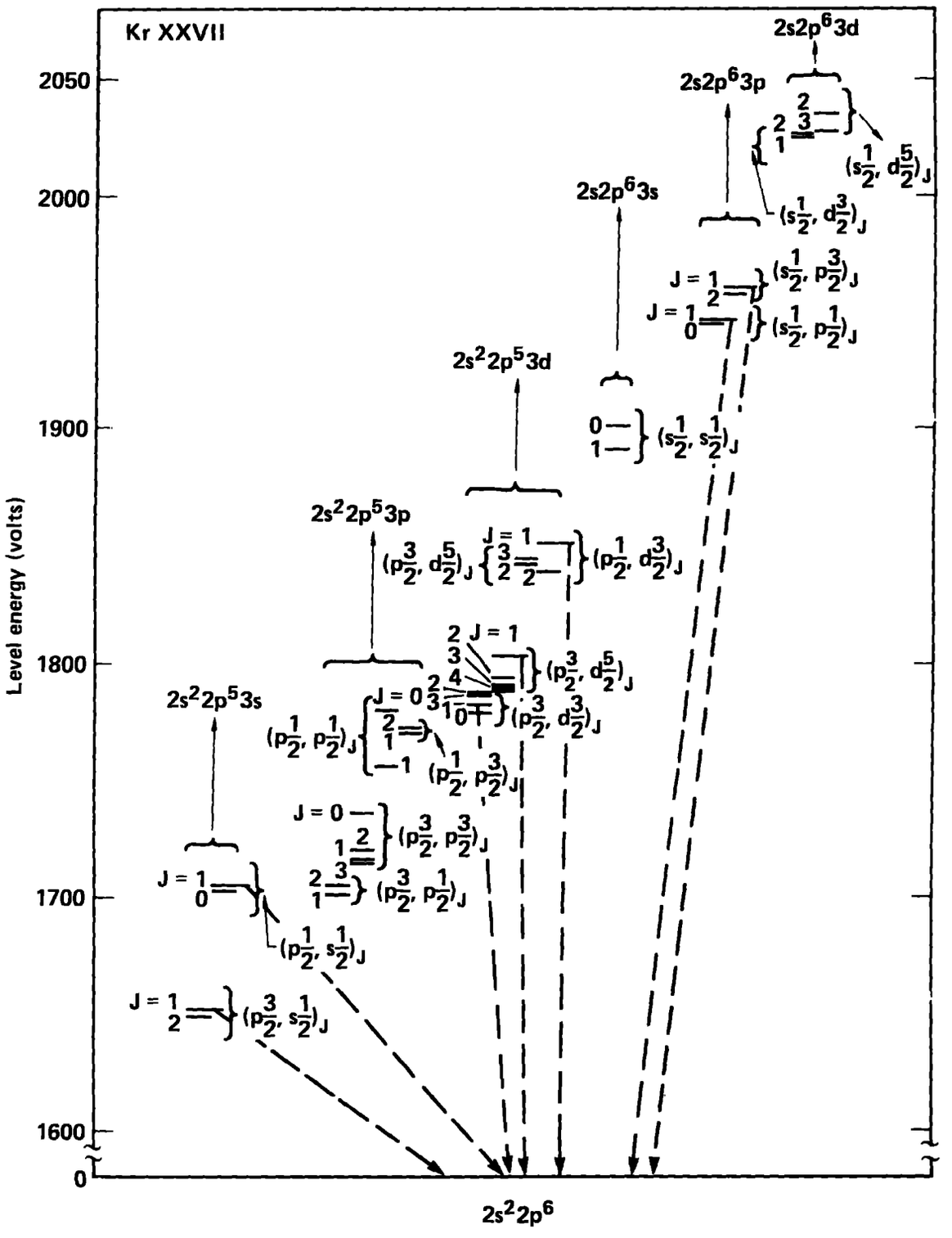

FIG. 3.3. The first 36 excited states of Ne-like krypton in JJ coupling.

TABLE 3.3. Some Neon–like Ion A–Values.

Ion	$A(2p^6 \leftarrow \Gamma)\ (sec^{-1})$ $\Gamma=(p_{3/2}, s_{1/2})_{1,lower}$	$\Gamma = (p_{3/2}, s_{1/2})_2$
Ne^{+0}	3.22 (7)*	7.6 (–2)
Ar^{+8}	4.64 (10)	2.89 (3)
Cu^{+19}	1.16 (12)	5.13 (5)
Ho^{+57}	9.86 (13)	1.55 (9)
U^{+82}	7.42 (14)	3.23 (10)

*3.22 (7) = 3.22×10^7

Inelastic Collisions at High Energy: Born's Method

At high collision energies it is easy to get approximate scattering cross sections from Born's formula. If the colliding particles interact via a potential V whose range is R, then "high energy" means

$$\hbar v_o \gg RV, \text{ or } (v_o/c) \gg (Z\alpha) \ . \tag{3.42}$$

The second exprrssion is for a Coulomb interaction between an incident electron and an ion. If we recall that bound electrons have speeds $v \sim Z\alpha c$, then it is apparent that the Born approximation essentially requires $v_o \gg v$ (bound e^-), for electron–ion scattering.

To obtain the Born cross section formula, we begin with Fermi's Golden Role, and note that the density of final states for the scattered particles is given by Eq. (3.8). Thus Eq. (3.15) is applicable. However the state $|\Gamma\rangle$ in that expression represents not only the target ion, but also must include the scattered particle. Born argued that if the velocity is high – or, equivalently, if the interaction is weak – then both the incident and final states of the scattered particle can be approximated as plane waves. Thus,

$$|\text{target} + \text{incident particle}\rangle \simeq e^{i\vec{k}_o \cdot \vec{r}} \; |\Gamma\rangle \; ,$$

$$|\text{target} + \text{scattered particle}\rangle \simeq e^{i\vec{k}_f \cdot \vec{r}} \; |\Gamma'\rangle \; , \tag{3.43}$$

where $\hbar k = \mu v$ for colliding particles having reduced mass μ. We now specialize to the case of e^-–ion scattering, for which

$$V(r) = -\frac{Z}{r} + \sum_{j=1}^{N} \frac{1}{|\vec{r} - \vec{r}_j|} \; . \tag{3.44}$$

When the product functions of Eq. (2.43) are used, one obtains, after some calculation, an interaction matrix element

$$4\pi \int_0^\infty dr \cdot r^2 \left[\frac{\sin Kr}{Kr}\right] \langle \Gamma' | V(r) | \Gamma \rangle \; ,$$

where $\hbar\vec{K} = \hbar(\vec{k}_f - \vec{k}_o)$ is the momentum transferred in the collision. With the interaction (3.44), the total Born cross section becomes, using Eq. (3.15),

$$\Gamma_{\Gamma'\Gamma}(k_o) = \frac{8\pi}{k_o^2} \int_{(k_o - k_f)}^{(k_o + k_f)} \frac{dK}{K^2} \left| \langle \Gamma' | \sum_{j=1}^{N} e^{i\vec{K} \cdot \vec{r}_j} \right| \Gamma \rangle |^2 \; . \tag{3.46}$$

Only for hydrogenic wave functions can the matrix element involving the bound electrons be evaluated exactly [see, e.g., M. Inokuti, Rev. Mod. Phys. 43, 297 (1971)].

Bethe derived a useful, simplified version of Eq. (3.46). He observed that the Born approximation implies

$$k_o - k_f \gtrsim 0 \; , \text{ and } k_o + k_f \gg 0 \; .$$

But, when K is large, the exponential oscillates and there is little contribution to the integral; when K is small the exponential can be expanded. If only the first term is kept, one obtains a dipole formula:

$$Q_{\Gamma'\Gamma}(k_o) \simeq \frac{8\pi}{3k_o^2} |\langle \Gamma' | \vec{D} | \Gamma \rangle|^2 \int_{k_o - k_f}^{\tilde{K}} \frac{dK}{K} \; , \tag{3.47}$$

where the upper limit of momentum transfer is ill-defined, except that we require $\tilde{K}(r_j) < 1$. Now, the square of the dipole matrix element is just the line strength factor S introduced in Eq. (3.32). Therefore, the cross section can be written in a form where it is proportional to the absorption oscillator strength:

$$Q_{\Gamma'\Gamma}(E_o) = \frac{2\pi f_{\Gamma'\Gamma}}{E_o \Delta E} \ln\left(\frac{2\tilde{K}E_o}{k_o \Delta E}\right) . \tag{3.48}$$

This is the Bethe-Born formula, expressed in terms of the incident energy E_o, and the excitation energy ΔE. In this equaton, all quantities are in atomic units, so the units of Q are $a_o^2 = 2.81 \times 10^{-17}$ cm^2.

Although this formula was obtained under the assumption that $E_o \gg \Delta E$, it is quite similar to an expression derived by Seaton [Atomic and Molecular Processes, ed. Bates (1962)] for low-energy electron-ion collisions, namely

$$Q_{\Gamma'\Gamma}(E_o) = \frac{2\pi f_{\Gamma'\Gamma}}{E_o \Delta E} \left[\frac{\pi}{\sqrt{3}} G^*\right] , \tag{3.49}$$

where G*, a quantity of order unity, is called an effective Gaunt factor. G*-values for several transitions (e.g., configuration→configuration) were determined by Blaha [Astrophys. J. 157, 473 (1969)], whose results are reproduced in Table 3.4.

That these two formulae are in reasonably good agreement with each other is somewhat surprising not only because of the different energy regimes for which they supposedly are valid, but also because of the fact that plane waves were used to derived the Bethe-Born formulae while Coulomb waves* were incorporated into Seaton's analysis.

Generally speaking these simple formulae can be used as a first guess – or a last resort. Better cross section values require more elaborate descriptions of the collision.

Inelastic Collisions at Low Energy: Coupled-Channels Methods

When the relative kinetic energy of the scattering particles is low, we expect atomic wave functions to be significantly perturbed during the collision. Thus, it is unlikely that a single product of (unperturbed) states – as assumed in Eq. (3.43) for Born's approximation – gives an accurate description. However, the wavefunction of the complete system of target ion plus scattered particle can always be expanded in terms of an infinite sum of product states,

*Coulomb waves are the positive energy solutions of the hydrogenic Schrödinger equation (2.1).

TABLE 3.4. Effective Gaunt factors G* for Threshold Excitation of Positive Ions.

Transitions	Z/k_o									
	2	3	4	5	6	8	10	12	14	16
$1s^2 2s–1s^2 2p$	520†	660	752	822	877	960				
$2s^2–2s2p$	640	708	771	830	876					
$2s^2 2p–2s2p^2$	690	753	808	856	898					
$2s^2 2p^2–2s2p^3$	710	774	821	863						
$2s^2 2p^3–2s2p^4$	723	776	824							
$2s^2 2p^4–2s2p^5$	711	765	816							
$2s^2 2p^5–2s2p^6$	703	762	809							
$2s^2 3s–2s^2 3p$		373	485	580	650	756	836	893	936	
$2p^6 3s–2p^6 3p$		525	600	657	707	786	845			
$3s^2–3s3p$		587	633	676	717	787				
$3s^2 3p–3s3p^2$		642	680	714	748	810				
$3s^2 3p^2–3s3p^3$		655	690	725	757	818				
$3s^2 3p^3–3s3p^4$		665	700	735	765	828				
$3s^2 3p^4–3s3p^5$		668	702	740	774	830				
$3s^2 3p^5–3s3p^6$		674	706	740	772					
$2s^2 3p–2s^2 3d$		320	450	552	640	764	853	904	954	974
$2p^6 3p–2p^6 3d$		446	544	617	677	778				
$2p^6 3s3p–2p^6 3s3d$		562	613	662	708	792				
$3s^2 3p–3s^2 3d$		524	593	651						
$2p^6 3p–2p^6 4s$			403							
$2p^6 3d–2p^6 4p$			440							
$3s^2 4s–3s^2 4p$		314	403	464						
$3s^2 3d–3s^2 4p$			478							

†Three figures behind the decimal point are given, e.g. 520 = 0.520.

$$\Psi(\vec{r}, \vec{r}_j) = \sum_{\Gamma''} \Phi_{\Gamma''}(\vec{r}_j)\,\phi_{\Gamma''}(\vec{r}) \ . \tag{3.50}$$

If the interaction V is weak, then only a few terms may actually be important. Of course, if the scattered particle, whose wave function is ϕ, is an electron, this equation must be modified to include exchange antisymmetry, i.e., each term becomes a Slater determinant. For the general arguments presented in this section, though, we can temporarily ignore this complication.

In Eq. (3.50), the states Φ_Γ represent eigenfunctions of the undisturbed target, and the ϕ_Γ represent the state of the (structureless) incident particle. Conventionally, each product state is called a scattering channel. Some straightforward mathematical manipulations (c.f. Mott and Massey, Ch. XIV) permit us to cast the time independent Schrödinger equation into the form

$$[\nabla^2 + k_\Gamma^2]\ \phi_\Gamma(\vec{r}) = \sum_{\Gamma''} \phi_{\Gamma''}(\vec{r})\, U_{\Gamma''\Gamma}(\vec{r}) \,, \tag{3.51}$$

where the $U_{\Gamma''\Gamma}$ are the so-called coupling matrix elements of the interaction,

$$U_{\Gamma''\Gamma}(\vec{r}) = \frac{2\mu}{\hbar^2} \langle \Gamma''(\vec{r}_j) | V(\vec{r}, \vec{r}_j) | \Gamma(\vec{r}_j) \rangle \ , \tag{3.52}$$

and where $E = E_\Gamma + \hbar^2 k_\Gamma^2/2\mu$ is the (constant) total energy. Formally, the scattering cross section for the transition $\Gamma \Rightarrow \Gamma'$ is gotten by matching the asymptotic form of $\phi_{\Gamma'}$ to

$$\phi_{\Gamma'}(\vec{r}) \underset{r\to\infty}{\sim} \frac{1}{r}\ e^{ik_f r}\ f_{\Gamma'\Gamma}(\hat{r}) \ . \tag{3.53}$$

Then, it can be shown that the differential scattering cross section, Eq. (3.10), is simply

$$I_{\Gamma'\Gamma}(\hat{r}) = \left(\frac{k_f}{k_o}\right) | f_{\Gamma'\Gamma}(\hat{r}) |^2 \tag{3.54}$$

The quantity $f_{\Gamma'\Gamma}$ is the scattering amplitude. (It is <u>unrelated</u> to the oscillator strength f introduced earlier.)

This is all straightforward, and no approximations have been introduced. The hitch (there always is a hitch) is that Eq. (3.51) represents an infinite set of coupled, second-order, inhomogeneous differential equations. In order of increasing severity, the approximations and simplifications commonly employed are:

Multi-state close coupling: retain just a few (~10) equations, including those for the initial and final states ϕ_Γ and $\phi_{\Gamma'}$, and those for states with large matrix elements $U_{\Gamma''\Gamma}$ and/or $U_{\Gamma''\Gamma'}$. Ignore all other matrix elements.

Two-state close coupling: retain just the four matrix elements ($U_{\Gamma\Gamma}$ $U_{\Gamma\Gamma'}$, $U_{\Gamma'\Gamma}$ $U_{\Gamma'\Gamma'}$) involving the initial and final states Γ and Γ'.

distorted-wave: make the two-state close coupling approximation. Then, assume that $|U_{\Gamma'\Gamma}| \ll |U_{\Gamma\Gamma}|$, so that the initial state wavefunction approximately satisfies the homogeneous equation

$$[\nabla^2 + k_o^2 - U_{\Gamma\Gamma}]\phi_\Gamma(\vec{r}) = 0. \tag{3.55}$$

Then, use this ϕ_Γ to solve the inhomogeneous equation

$$[\nabla^2 + k_f^2 - U_{\Gamma'\Gamma'}]\phi_{\Gamma'}(\vec{r}) = \phi_\Gamma U_{\Gamma\Gamma'} \tag{3.56}$$

for$\phi_{\Gamma'}$, and obtain the cross section $\Gamma \Rightarrow \Gamma'$ from Eqs. (3.53) and (3.54). We can ultimately reduce the coupled-channel calculation to a Born-like calculation, which amounts to solving the single equation

$$[\nabla^2 + k_f^2]\phi_{\Gamma'}(\vec{r}) = e^{i\vec{k}_o \cdot \vec{r}} U_{\Gamma\Gamma'} \quad . \tag{3.57}$$

In fact, the Born formula discussed previously is a first-order approximation of the true solution of Eq. (3.57); consequently, collision physicists refer to it as the "first" Born approximation.

Collision Strengths and Their Properties

Upon allowing for target state degeneracies, the e^--ion cross sections of Eqs. (3.47) - (3.49) all exhibit the form

$$Q_{\Gamma'\Gamma} \propto \frac{1}{g_\Gamma k_o^2} \quad .$$

It turns out to be convenient to use this fact, and thereby to define a quantity Ω called the collision strength;

$$\Omega_{\Gamma'\Gamma} = \frac{\pi}{k_o^2 g_\Gamma} \Omega(\Gamma',\Gamma) \ , \tag{3.58}$$

which is dimensionless, and is symmetrical in its arguments, i.e., $\Omega(\Gamma',\Gamma) = \Omega(\Gamma,\Gamma')$. If the logarithmic behavior of the Bethe–Born formula is to be believed, then the collision strength is only weakly dependent on the energy $E_o = \frac{1}{2}k_o^2$. In fact, since their introduction some 40 years ago, many physicists have steadfastly held this opinion. Only within the past few years has it become commonly accepted that collision strengths can have a significant energy dependence. For the L–S coupling scheme, one has [see R. Henry, Physics Reports 58, 1 (1981)]

$$\Omega(\Delta L = 1, \Delta S = 0) \sim \ell n(E_o/\Delta E) \tag{3.59a}$$

$$\Omega(\Delta L \neq 1, \Delta S = 0) \sim \text{constant} \tag{3.59b}$$

$$\Omega(\Delta S \neq 0) \sim (\Delta E/E_o)^2 \tag{3.59c}$$

A comparable set of rules does not exist for jj coupling. However, the energy dependence of any particular collision strength can be found via a recoupling: each jj state corresponds to an admixture of LS states

$$|(j_1 j_2) J\rangle = \sum_{LS} (\text{coupling coefficients}) \ | \ LSJ \rangle \ , \tag{3.60}$$

and so one has, conceptually,

$$\Omega^{(jj)} = \sum_{LS} (\text{re–coupling coefficients for } \Gamma) (\text{re–coupling coefficients for } \Gamma') \ \Omega^{(LS)} \tag{3.61}$$

Documented computer programs exist to carry out this task.

Some Z–scaling properties of collision strengths are quite simple. In the absence of angular momentum recoupling effects (i.e., in strict LS coupling), and at an energy well above threshold one has

$$Z^2\Omega \approx \text{constant.} \tag{3.62}$$

As an example of how the breakdown of LS coupling affects Ω–values, we consider the simple He–like case $1s^2 \rightarrow (1s2p)\ ^3P_1$. At low Z the collision strength has the form (3.59c), but as Z increases the spin orbit interaction mixes singlet and triplet states, so the logarithmic form (3.59a) also contributes; this behavior is evident in Fig. 3.4, where scaled collition strengths are plotted versus Z for different values of the energy parameter $\chi = E_o/\Delta E$. As an example of the scaling behavior (3.62), in Fig. 3.5 we show collision strengths for the Na–like ion transition 3s → 3p. No mixing effects are present for this case. It is apparent that Eq. (3.62) is valid only at collision energies satisfying $\chi \geq 10$.

Some general references for Ω–values are:

1. the review by R.J.W. Henry, cited above (1981).
2. a LASL Informal Report #LA–8267–MS (1980).
3. a continuing series of papers by D. Sampson and collaborators, usually in Astrophys. J. (1976 – present).

For Ne–isoelectronic sequences ($Z \leq 50$), one can consult recent work by K. Reed and A. Hazi (Phys. Rev., and unpublished LLNL reports).

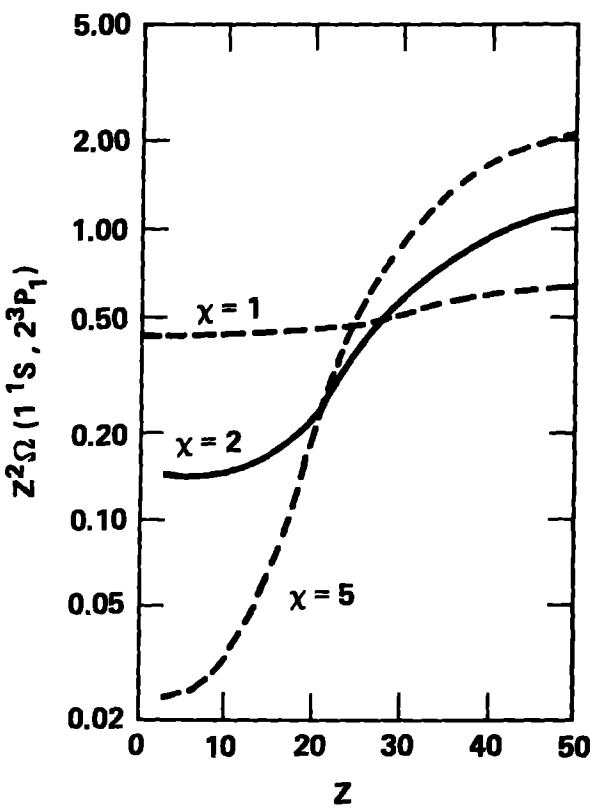

FIG. 3.4. Intermediate coupling effects in Sampson's data for the Helium sequence.

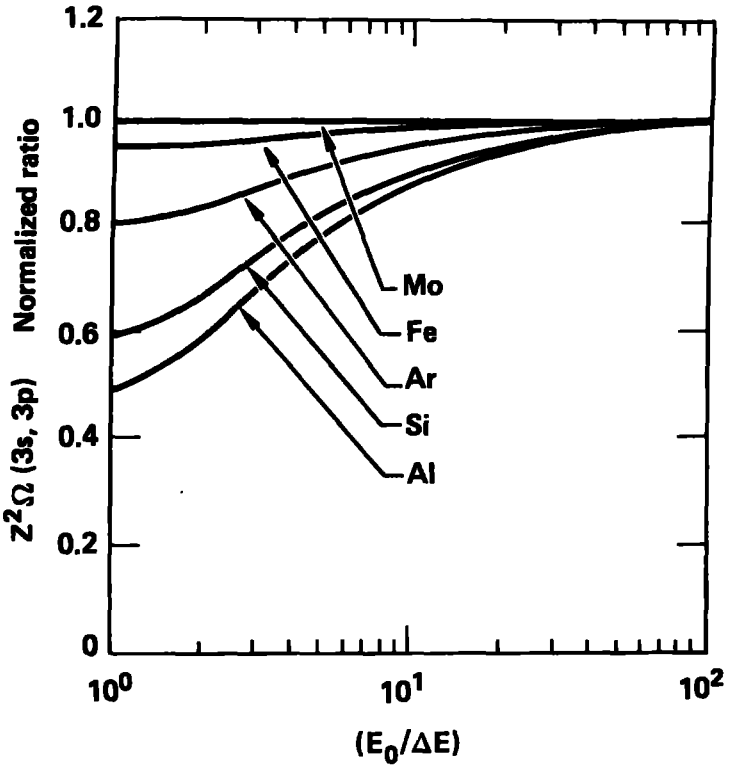

FIG. 3.5. Collision strengths of J. B. Mann for the sodium sequence, normalized to the Mo-values (from 1980 LASL report #LA-8267-MS).

Comments on Relativistic Effects in Collisions

Relativity can alter scattering cross sections in a variety of ways:

(1) modification of target wavefunctions;

(2) use of Dirac, instead of Coulomb, waves to represent incident e^-;

(3) kinematic effects (e.g., $\hbar k = \gamma m_e v$, with $\gamma^{-2} = 1 - v^2/c^2$).

For a recent discussion of these topics, the interested reader should consult B. L. Moiseinvitsch, Adv. Atomic & Molecular Physics 16 (1980). For plasmas in which the ionization state has been achieved primarily through photoionization – as opposed to thermal, collisional ionization – the third item is less important than the first two, since mean thermal electron energies will be somewhat less than the atomic ionization energies, viz. $(kT/m_e) < (Z\alpha c)^2$.

As an illustration of the magnitude of items 1 and 2, Table 3.5 compares some Z-scaled collision strengths for hydrogenic ions. Those labeled CB were computed in a (Coulomb) Born approximation, while those labeled RCB were computed in a Born

approximation, but using Dirac bound and free orbitals. Spin–orbit effects were included in the electron–electron interaction, but retardation effects (e.g., Breit interaction) were not. These are the only results, of which I am aware, for relativistic e^-–ion collision strengths.

As a last point, we note that Jones [Phil. Trans. Royal Soc. (London), A277, 587 (1975)] showed that, to order $(Z\alpha)^2$, the Breit interaction does not affect term LS values, Ω(LS, L'S'), but of course does modify values for transitions to and from specific fine-structure levels, Ω(LSJ, L'S'J').

TABLE. 3.5. Values of $Z^2\Omega$ for Hydrogenic Ions[a].

	$Z^2\Omega$(1s, 2s)		$Z^2\Omega$(1s, 2p)	
Z	CB[b]	RCB[c]	CB[b]	RCB[c]
2	0.797	0.792	3.37	3.39
25	0.88	0.93	4.06	4.04
50	0.88	1.15	4.09	4.06
100	0.88	2.75	4.10	3.41

a All calculations are for $\xi_1/|E_1| = 1$ where ξ_1 is the energy of the colliding electron when the target is in the ground state; E_1 is the energy of the ground state.
b CB Results of A. Burgess, et al. (1970), Phil. Trans. Roy. Soc. 266, 225.
c RCB Results of R. W. Walker (1974), J. Phys. B. 7, 97.

LECTURE #4 – IONIZATION BALANCE; SPECTRAL LINE SHAPES

Until now, we have only treated transitions between states of the same ionic specie. In this lecture, we extend the discussions of collisional and radiative transitions to include ionization and recombination processes. Then, we will briefly describe various ionization equilibria. Finally, we will sketch some basic ideas on the subject of spectral line shapes. In contrast to the first two lectures, we will use natural units most of the time.

Photoionization

Whenever an atom absorbs a photon of energy $\hbar\omega$ greater than the binding energy of one of its electrons, the process of photoionization occurs,

$$\hbar\omega + \text{atom}(\Gamma) \rightarrow e^- + \text{ion}(\Gamma') \ .$$

The cross section for this process can be determined from Fermi's Golden Rule, but to do so we must assemble several bits of information:

$$\text{Photon flux} = \frac{U_\omega c}{\hbar\omega} = \left(\frac{1}{\pi c}\right)^2 \frac{1}{2} N_\omega \ . \tag{4.1}$$

$$\text{Energy of ejected electron} = \epsilon = \frac{1}{2} m_e v^2 = \hbar\omega - (E_\Gamma - E_{\Gamma'}) \ . \tag{4.2}$$

$$\text{Orbital of ejected electron} = \phi_{\epsilon \ell m}(\vec{r}) = \sqrt{\hbar}\,\frac{1}{r} P_{\epsilon \ell}(r)\, Y_{\ell m}(\hat{r}) \ . \tag{4.3}$$

With the normalization $\langle \frac{1}{r}P_{\epsilon'\ell} | \frac{1}{r}P_{\epsilon\ell} \rangle = \delta(\epsilon'-\epsilon)$, Eq. (4.3) represents an outgoing flux of one electron.

Upon combining these results in the formula for the absorption probability per unit time, Eq. (3.29), we get the photoabsorption cross section ($\Gamma \rightarrow \Gamma'$)

$$\sigma_{\Gamma',\Gamma}(\omega) = \frac{4\pi^2 \omega}{3\hbar c} \left| \langle \Gamma' | \vec{D} | \Gamma \rangle \right|^2 \ . \tag{4.4}$$

[Often, the factor $\hbar$ arising from Eq. (4.3) is extracted and used to cancel the factor $\hbar^{-1}$ in Eq. (4.4). And, since the final state is fixed by the photon energy, it sometimes suffices

to denote just the initial state.] This is an E1 transition formula, and so the selection rules given in the Table 3.1 apply.

Even for hydrogenic systems, the evaluation of bound–free matrix elements $\langle \epsilon'\ell' | r | n\ell \rangle$ is non–trivial. Analytic formulae have been published only for atomic states with $n\ell \leq 4p$. Detailed discussions can be found in: H. Hall (1936) Rev. Mod. Phys. 8, 358; J. M. Harriman (1956), Phys. Rev. 101, 592; and A. Burgess (1964), Mem. Royal Astron. Soc. 69, 1. Some hydrogenic results of Burgess are shown in Fig. 4.1. In particular, the difference in the 2s and 2p cross sections should be noted: this difference is at the heart of a laboratory soft x–ray laser scheme proposed by P. Hagelstein (cf. his Ph.D. thesis, Lawrence Livermore National Laboratory, Livermore, CA, UCRL–53100).

For most purposes, it is sufficient to use semi–classical formulae derived by Kramers, which have no dependence on orbital quantum number ℓ:

$$\sigma_n^{(K)}(\omega) = \frac{64\pi}{3\sqrt{3}}\left(\frac{\alpha a_o^2 n}{Z^2}\right)\left(\frac{\omega_n}{\omega}\right)^3 = \frac{7.9 \times 10^{-18} n}{Z^2}\left(\frac{\omega_n}{\omega}\right)^3 \ \text{cm}^2 \qquad (4.5)$$

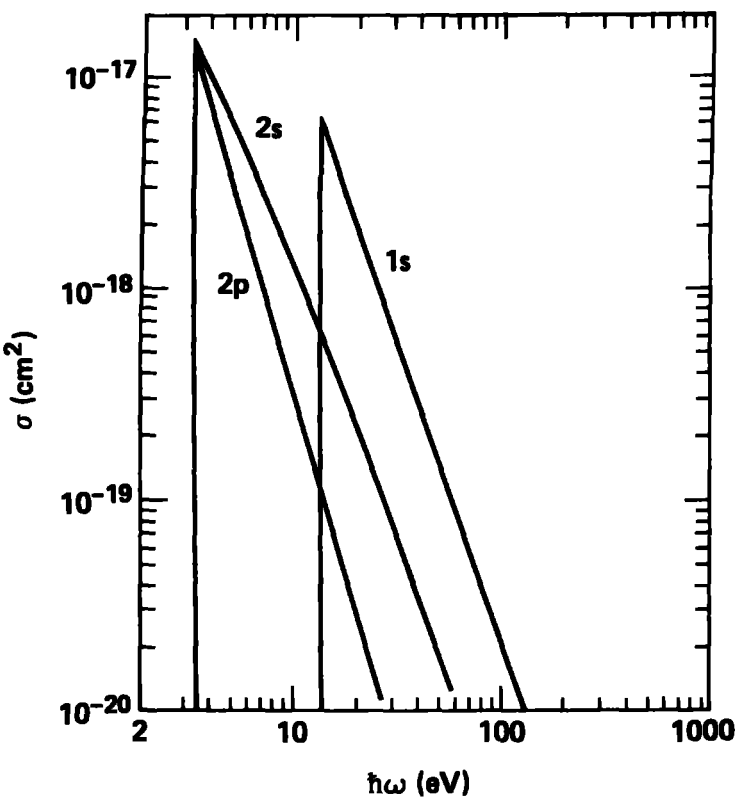

FIG. 4.1. Cross section for $H(n\ell) + \hbar\omega \rightarrow H^+ + e$ (based on the matrix elements tabulated by A. Burgess).

In this formula, $\hbar\omega_n = (Z^2/n^2)$ Ryd. is the electron's binding energy. Corrections to the Kramers formula are usually given in terms of a "Gaunt factor" $G_{n\ell}(\omega)$, such that

$$\sigma_{n\ell}(\omega) = \sigma_n^{(K)}(\omega)\, G_{n\ell}(\omega) \ . \tag{4.6}$$

Table 4.1 lists threshold values, $G_{n\ell}(\omega_n)$, and frequency–averaged values.

Photoionization cross sections for complex systems (more than one bound electron) invariably are computed using central field wave functions. Two useful compilations of theoretical results for $Z \leq 30$ are: W. D. Barfield, G. D. Koontz and W. F. Huebner (1972), J. Quant. Spectrosc. Radiative Transf. 12, 1409; and R. F. Reilman and S. T. Manson (1979), Astrophys. J. Suppl. 40, 815. The first of these gives fitting coefficients for polynomial expressions computed using Dirac–Slater wavefunctions. The second tabulates σ–values computed using Hartree– Slater wavefunctions. Typically, the accuracy of such calculations is judged to be better than 20%.

As a last comment on the subject of dipole (E1) photoionization, it is worth mentioning a parametric form introduced into the astrophysical literature by Seaton in the 1960's:

$$\sigma(\omega) = \sigma(\omega_o)\, [\, (\omega/\omega_o)^s \beta + (\omega/\omega_o)^{s+1} (1-\beta)\,] \ , \tag{4.7}$$

TABLE 4.1. Gaunt factors for hydrogen atom.

Orbital	G at absorption edge		$\bar{G}$ for whole continuum	
1s		0.80		0.84
2s	0.96	0.89	1.20	0.94
2p	0.88		0.83	
3s	1.14		1.6	
3p	1.14	0.92	1.31	0.99
3d	0.73		0.64	
4s	1.3	0.94	1.95	
4p	1.3		1.74	1.01
4d			1.18	
4f			0.43	
5		0.95		1.02
6		0.96		1.02
7		0.97		1.02

with $\hbar\omega_o$ being the ionization threshold. It is more flexible than Kramer's formula and actually fits light ion cross sections fairly well near threshold. Also, it is very convenient for computations.

Relativistic effects in atomic photoionization are of two kinds. One arises from the use of relativistic bound and free electron wavefunctions, and is a fairly straightforward generalization of formulae presented here. The other occurs when the photon energy is very large, say $\hbar\omega \geq m_e c^2$, and then the dipole approximation is no longer valid. These issues are discussed at length in Hall's paper, and also are treated in Bethe and Salpeter. The report UCRL–51326 (J. H. Scofield, 1973) tabulates relativistic neutral atom cross sections for the entire periodic table for 1–1500 keV photons.

The rate (ionizations/atom/time) at which photoionization occurs in the presence of a radiation field having a specific energy density U_ω (energy/volume/angular frequency interval) is just

$$F_\Gamma = c \int_{\omega_o}^{\infty} U_\omega \frac{\sigma_\Gamma(\omega)}{\hbar\omega} d\omega \ . \tag{4.8}$$

As an example, we can compute the ionization rate for a hydrogenic atom in a black–body radiation field, using Kramer's formula. The result is

$$\text{KRAMERS } F_n = \left\{ \frac{8\alpha^4 c}{3\sqrt{3}\ \pi a_o} \right\} \left(\frac{Z^4}{n^5} \right) \int_1^{\infty} \frac{dx}{x} [\exp(\hbar\omega / k_B T_{rad}) - 1]^{-1} \ ; \tag{4.9}$$

here, the numerical coefficient { } has the value 7.98×10^9/sec, and T_{rad} is the radiation temperature. More often than not, U_ω is not thermal, and so one usually deals directly with cross sections.

Radiative Recombination

This is the inverse of photoionization; thus, we can use the principle of detailed balance to relate the cross sections for these two processes. We use Eq. (3.16), but expressed in terms of photon and electron momenta, $\hbar k$ and $\hbar q = m_e v$, to write the recombination cross section ($\Gamma' \to \Gamma$) as

$$a_{\Gamma\Gamma'}(q) = k^2 g_\Gamma \sigma_{\Gamma'\Gamma}(k) / q^2 g_{\Gamma'} \ . \tag{4.10}$$

Note that we have to specify the state Γ' of the recombining ion.

There is no need to dwell on this formula, as all of our discussion of photoionization cross sections applies here too. However, in contrast to the comment about photoionization rates, more often than not plasma species {"x"} have speed distributions $D_x(v)$ that are thermal. Therefore, it is thermal recombination rate coefficients,

$$\beta^{(rad)}_{\Gamma\Gamma'}(T_e) = \langle a_{\Gamma\Gamma'}(v) \cdot v \rangle$$

$$= \int_0^\infty D_e(v)\, a_{\Gamma\Gamma'}(v)\, v\, dv \qquad (4.11)$$

that one usually requires. At plasma temperatures $k_B T \leq$ a few tens of kilovolts, relativistic effects are negligible and one has Maxwell–Boltzmann distributions,*

$$D_x(v) = 4\pi v^2 (m_x/2\pi k_B T_x)^{3/2} \exp(-m_x v^2/2k_B T_x) \ . \qquad (4.12)$$

Suppose we adopt the Kramers formula for photoionization. Then, using Eqs. (4.10) – (4.12), we get for the radiative recombination rate coefficient (ion → n)

$$\text{KRAMERS}\quad \beta^{(rad)}_n(T_e) = \frac{64Z\alpha^4 a_o^2 c\sqrt{\pi}}{3\sqrt{3}\, g_{ion}} \left(\frac{\hbar\omega_n}{k_B T_e}\right)^{1/2} \xi\left(\frac{\hbar\omega_n}{k_B T_e}\right)$$

$$= 5.21 \times 10^{-14} \left(\frac{Z}{g_{ion}}\right) \left(\frac{\hbar\omega_n}{k_B T_e}\right)^{1/2} \xi\left(\frac{\hbar\omega_n}{k_B T_e}\right) \text{cm}^3/\text{sec} \ , \qquad (4.13)$$

where $\xi(x) = xe^x E_1(x)$ involves the first exponential integral function; when $x \gg 1$, $\xi(x) \to 1$. The Z–scaling properties of this formula are readily determined. The binding energy $\hbar\omega_n \propto Z^2$, so we have

$$\beta^{(rad)}_n(Z,T) = Z\beta^{(rad)}_n(1, T/Z^2) \ . \qquad (4.14)$$

Most plasma modelling calculations make the approximation that excited–state recombination rate coefficients are given by Eq. (4.14); only for the ground state is a more accurate photoionization cross section used. The astrophysical literature contains primarily coefficients that have been summed over all states of the recombined ion. For

*Some aspects of relativistic reaction rates have been discussed by T. A. Weaver (1976), Phys. Rev. A 13, 1563.

light ions, Z<26, two papers are especially recommended: C. B. Tarter (1971), Astrophys. J. 168, 313; (1973), ibid 187, 607); and S. M. V. Aldrovandi and D. Pequignot (1973), Astron. and Astrophys. 25, 137.

General trends for hydrogenic ions are illustrated in the accompanying Tables 4.2 and 4.3. In particular, one should note that individual $\beta_{n\ell}$-values, gotten from true hydrogenic cross sections, are not proportional to $(2\ell+1)$.

Thermal Photoionization Equilibrium

Let's apply these results to the simple problem of a plasma in which matter and radiation have the same temperature, i.e., the plasma is in thermal equilibrium. Because of the equilibrium conditions, we know that every reaction is balanced exactly by its inverse. For the photoionization problem we have, then,

$$N_e N_{ion} \beta_\Gamma^{(rad)} = N_\Gamma F_\Gamma \ . \tag{4.15}$$

TABLE 4.2. Summed recombination rate coefficients for H-like ions, in units 10^{13} cm^3 sec^{-1}.

	T				
	1250°K	2500°K	5000°K	10,000°K	20,000°K
$\alpha_A = \sum_1^\infty \alpha_n$	17.4	11.0	6.82	4.18	2.51
$\alpha_B = \sum_2^\infty \alpha_n$	12.8	7.72	4.54	2.60	1.43
$\alpha_C = \sum_3^\infty \alpha_n$	10.3	5.99	3.37	1.83	0.950
$\alpha_D = \sum_4^\infty \alpha_n$	8.65	4.86	2.64	1.37	0.683

TABLE 4.3. Radiative recombination rate coefficients, at T=10,000K, for $H^+ + e \rightarrow H(n,\ell) + \hbar\omega$, in units 10^{-16} $cm^3 sec^{-1}$ [obtained from functions tabulated by Burgess (48)].

n \ ℓ =	0	1	2	3	4	5	6	7	8	9	10	11
1	1582											
2	234	536										
3	78.2	204	173									
4	36.3	96.5	109	55.5								
5	19.9	52.8	66.9	49.4	17.9							
6	12.2	31.6	42.9	37.5	20.5	5.85						
7	7.94	20.3	28.8	28.2	18.7	8.22	2.00					
8	5.48	13.7	20.0	20.9	15.8	8.59	3.25	0.706				
9	3.94	9.73	14.4	15.6	12.8	7.97	3.75	1.28	0.259			
10	2.93	7.09	10.6	12.0	10.5	7.12	3.83	1.61	0.502	0.100		
11	2.23	5.34	7.94	9.15	8.45	6.20	3.67	1.77	0.688	0.203	0.039	
12	1.74	3.99	6.08	7.22	6.85	5.38	3.41	1.83	0.825	0.304	0.084	0.016

But in equilibrium, there also is the Saha equation,

$$\frac{N_e N_{ion}}{N_\Gamma} = \left(\frac{2g_{ion}}{g_\Gamma}\right)\left(\frac{m_e k_B T}{2\pi\hbar^2}\right)^{3/2} \exp\left(\frac{-I_\Gamma}{k_B T}\right) \quad , \tag{4.16}$$

that relates the density of ionized atoms to that of atoms in a state with ionization potention I_Γ. If we use the Saha expression to eliminate the densities from Eq. (4.15), we obtain the result that the ratio $F_\Gamma/\beta_\Gamma^{(rad)}$ equals the right hand side of Eq. (4.16).

After putting $g_n = 2n^2$, we can check this against the expression we get by using Kramers hydrogenic cross section formula. The do not agree! The discrepancy can be traced, not to our choice of an approximate cross section (detailed balancing holds, no matter how stupid we are), but to the fact that radiative recombination is a photoemission process – in addition to the spontaneous rate (4.11), there is a term corresponding to stimulated recombination that is proportional to the radiation energy density U_ω. We find that the cross section for recombination, Eq. (4.10), must be multiplied by the factor

$$1 + \frac{1}{2} N_\omega = 1 + \frac{\pi^2 c^3}{\hbar\omega^3} U_\omega \quad , \tag{4.17}$$

which for a black-body field is just $[1-\exp(-\hbar\omega/k_B T)]^{-1}$. Most of the time, this correction – which invariably is <u>not</u> included in tabulated recombination rate coefficients – is small

and can be neglected; but, clearly, one can think of instances where the correction will be important.

Electron Impact Ionization

We now turn our attention to the process of collisional ionization,

$$\text{ion}(Z,\Gamma) + e^- \text{ (energy} = \epsilon) \rightarrow \text{ion}(Z+1, \Gamma') + 2e^- \ ,$$

which was first treated by Thomson in 1912. He used an impact parameter formulation [cf. Eq. (3.12)], and set the ionization probability equal to 1 or 0 according to whether the maximum energy transferrable to a stationary electron,

$$\Delta\epsilon = \epsilon / [1 + b^2 \epsilon^2] \ , \tag{4.18}$$

is greater than or less than the electron's binding energy. (In this equation, all quantities are in atomic units.) This prescription yields an ionization cross section (at. units)

$$\text{THOMSON} \quad Q_\Gamma^{\text{ion}}(\epsilon) = \frac{\pi}{I_\Gamma \epsilon} \left(1 - \frac{I_\Gamma}{\epsilon}\right) \ . \tag{4.19}$$

In the 1960's this classical scheme was extended by Gryzinski, by Stabler, and by Garcia to include the effects of the bound electron's motion. Whereas Thomson's formula is seldom very accurate, Gryzinski-type formulae are fairly accurate at high energies.

It should come as no great surprise that the Born approximation also is accurate at high energies. This is confirmed for hydrogen in Fig. 4.2. Even better is the so-called Glauber approximation, which is another high-energy formula. On the other hand, Bethe's version of the Born approximation, which also has a $(\ell n \epsilon)/\epsilon$ behavior, is poor except at very high energies, $\epsilon \geq 1$ keV.

Glauber-type calculations have not been carried out for complex ions, and so some reasonably accurate general formula is needed for low-energy collisons. The most often used formula is due to Lotz (1967, Astrophys. J. Suppl. 14, 207). Writing I_H for 1 Rydberg (=13.606 eV), his cross section expression is

$$\text{LOTZ} \quad Q_\Gamma^{\text{ion}}(\epsilon) = 2.4 \times 10^{-16} \left(\frac{I_H}{\epsilon}\right) \left(\frac{I_H}{I_\Gamma}\right) \ell n \left(\frac{\epsilon}{I_\Gamma}\right) \ \text{cm}^2 \ . \tag{4.20}$$

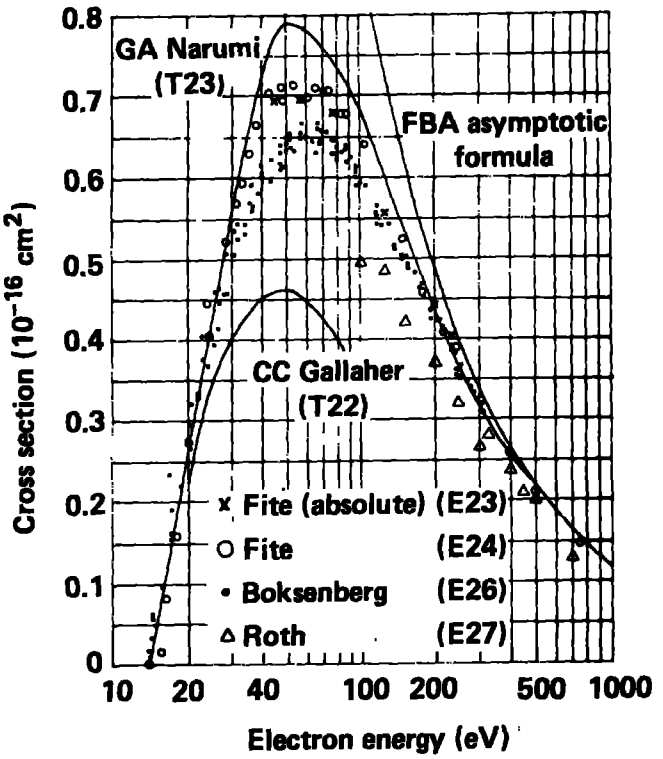

FIG. 4.2. Cross section for ionization. $e + H(1s) \rightarrow e + H^+ + e$. [Figure from I.P.P. Nagoya University Report #IPPJ–DT–48 (1978).]

This simple formula gives amazingly good agreement with a large set of data, typically being accurate to within a fraction of two at all energies.

Within the last few years, more extensive ionization data have become available, and requirements for cross section accuracy have stiffened. Crandall and collaborators (ORNL) have carefully measured the ionization cross sections for ground–state Li–like ions C^{+3}, N^{+4} and O^{+5}. Their C^{+3} data are compared with several formulae in Fig. 4.3. Among the theoretical advances, the work of Yonager (NBS and now LLNL) is particularly noteworthy. He has performed an extensive series of ionization calculations within the distorted wave approximation. His results should be the best available for highly–charged ions.

A brief status report of this field is given by: S. M. Younger (1982), Comments Atom. & Molec. Phys. 11, 193. Data for Ne–like ions was published in: S. M. Younger (1981), Phys. Rev. A23, 1130.

Thermal rate coefficients for collisional ionization can be computed straightforwardly, once one has the cross section. For the simple Lotz formula we obtain

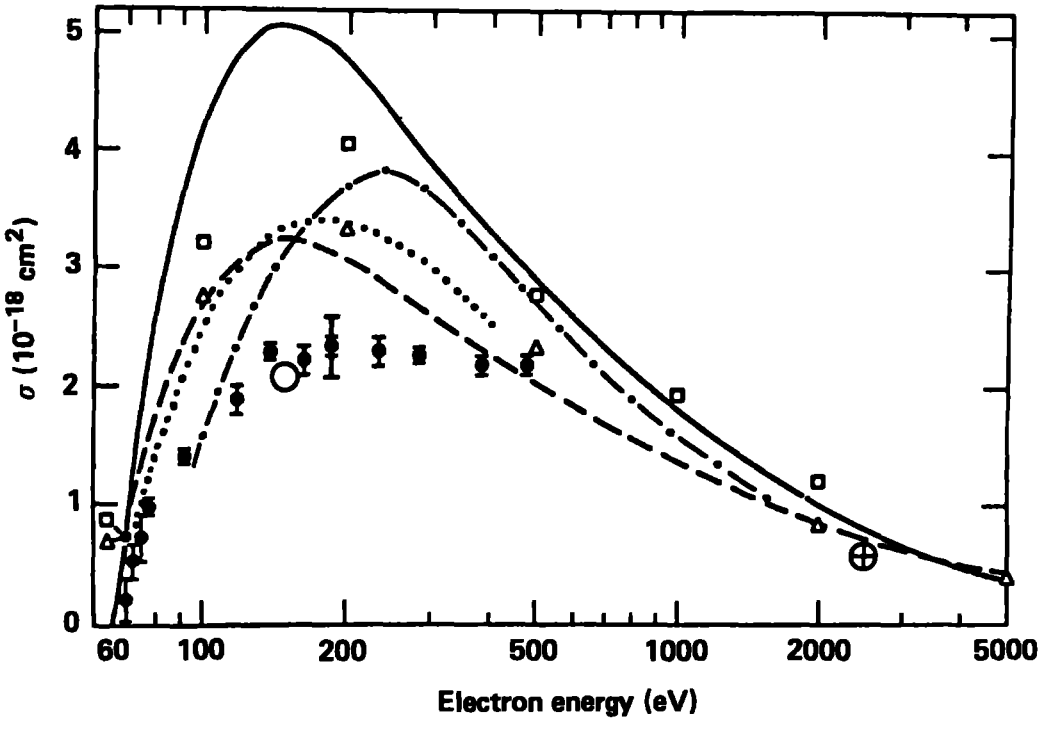

FIG. 4.3. Cross sections for electron–impact ionization of C^{3+} as a function of electron energy. Crandall, et al., ●; result inferred from rate measurement by Kunze, O; result of Donets, ⊕; semiempirical estimate due to Lotz, □; ECIP value by Barfield, Δ; classical theory of Salop, solid curve; Coulomb–Born calculation of Moores, dotted curve; scaled Coulomb–Born value according to Golden and Sampson, dashed curve; modified Bethe approximation of Hahn, dot–dashed curve. Error bars are 2 standard deviations on counting statistics except heavy bar at 187 eV is absolute total uncertainty estimated at good confidence. [Figure taken from Crandall et al., 1978, Phys. Rev. A18, 1911.]

$$\text{LOTZ}\quad C_\Gamma^{(\text{ion})}(T_e) = \langle \text{LOTZ}\quad Q_\Gamma^{(\text{ion})}(v) \bullet v \rangle$$

$$= 6.0 \times 10^{-8} \left(\frac{I_H}{I_\Gamma}\right)\left(\frac{I_H}{k_B T_e}\right)^{1/2} E_1\left(\frac{I_\Gamma}{k_B T_e}\right) \text{cm}^3/\text{sec} \ . \qquad (4.21)$$

Hydrogenic levels have ionization potentials $I_\Gamma \sim Z^2$, so the scaling of $C^{(\text{ion})}$ with Z is

$$C^{(\text{ion})}(Z,T) = Z^{-3}\, C^{(\text{ion})}(1, T/Z^2). \qquad (4.22)$$

Three–Body Recombination

Being the inverse of electron–collisional ionization, this process has a cross section $Q^{(3B)}$ that is related to $Q^{(ion)}$ through detailed balancing. However, of more practical interest the rate coefficient,

$$C_\Gamma^{(3B)} = \langle Q_\Gamma^{(3B)}(v) \bullet v \rangle \ . \tag{4.23}$$

If we again restrict ourselves to thermal velocity distributions, the quantity $C_\Gamma^{(3B)}(T_e)$ can be related to the thermal ionization rate coefficient through the Saha equation since, in equilibrium, one has

$$N_e^2 N_{ion} C_\Gamma^{(3B)}(T_e) = N_e N_\Gamma C_\Gamma^{(ion)}(T_e) \ . \tag{4.24}$$

For Lotz's ionization cross section it follows that

$$\text{LOTZ} \quad C_\Gamma^{(3B)}(T_e) = 2.0 \times 10^{-31} \left(\frac{g_\Gamma}{g_{ion}}\right)\left(\frac{I_H}{k_B T_e}\right)^{3/2}\left(\frac{I_H}{I_\Gamma}\right)^2 \xi\left(\frac{I_\Gamma}{k_B T_e}\right) \text{cm}^6/\text{sec} \ , \tag{4.25}$$

where ξ is defined in the text following Eq. (4.13). In this case the Z–scaling is

$$C^{(3B)}(Z,T) = Z^{-7}\, C^{(3B)}(1, T/Z^2) \tag{4.26}$$

Also, note that $C_n^{(3B)} \sim n^6$, so three–body recombination becomes increasingly more important for higher levels n.

Autoionization

In order to understand the remaining ionization balance processes, we need to describe autoionization. A good example is provided by the Li–ion sequence.

Ordinarily, atomic spectra arise from ions in which only a valence electron is excited above the ground state. But, suppose that an inner electron were excited; for Li–like ions, the lowest such states arise from the configurations $(1s2\ell 2\ell')$. As illustrated in Fig. 4.4, these levels lie far above the ground state of ionized lithium, and therefore are degenerate with states of the $(Li^+ + e^-)$ system. Quantum mechanics tells us that a time–independent perturbation V, with a non–zero matrix element $\langle 1s2\ell 2\ell' | V | 1s^2, \epsilon\ell'' \rangle$, can cause a transition between such degenerate states at a rate given by Fermi's Golden Rule, Eq. (3.9). But, only an interaction involving two electrons can cause such a

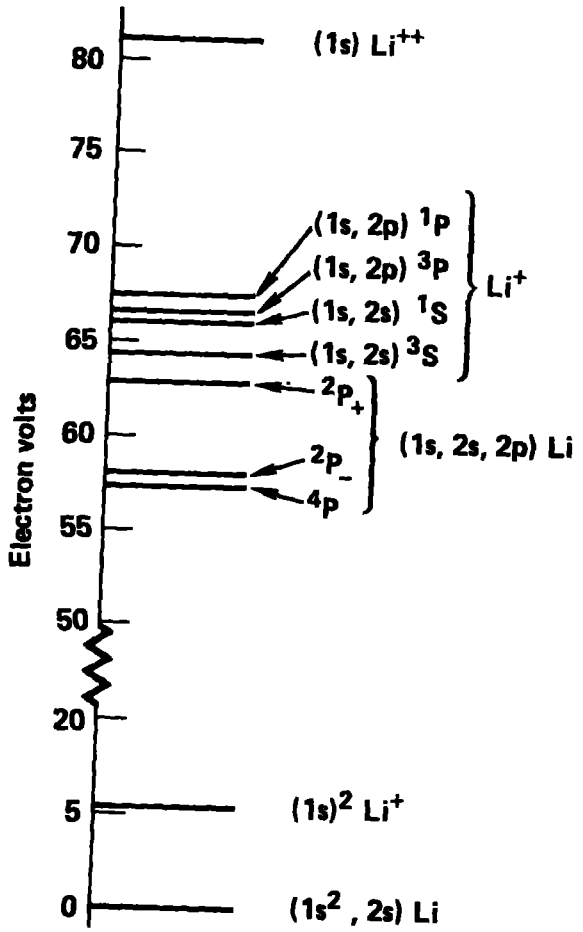

FIG. 4.4. Partial energy level diagram for states of Li and Li^+.

transition, because the initial and final states differ by two orbitals. Thus, the atom "auto–ionizes", with a probability

$$W^{(a)} = \frac{2\pi}{\hbar} \left| \langle \text{ion} + e^- \left| \sum_{i \neq j} r_{ij}^{-1} \right| \text{inner–shell hole} \rangle \right|^2 \rho(\epsilon) \tag{4.27}$$

When relativistic effects are important (e.g., high–Z systems), one must replace $1/r_{ij}$ by the Breit operator, Eq. (2.51).

The Auger effect relates to the same physical process, namely a radiationless re–arrangement involving the ejection of one (or more) bound electrons. However, that terminology usually is applied to the sequence of events that occurs after an inner–shell electron has been ionized. Therefore, analogous to the Li–atom example, above, would be the reaction sequence

$$\begin{aligned} \text{Be}(1s^2 2s^2) + \hbar\omega &\rightarrow \text{Be}^+(1s2s^2) + e^-(\text{photo}) \\ &\hookrightarrow \text{Be}^{++}(1s^2) + e^-(\text{Auger}) \end{aligned}$$

In particular, note that the photoelectron has an energy related to $\hbar\omega$, but that the Auger electron has an energy equal to the difference of the Be^{+} and Be^{++} states.

In many-electron systems, several electrons may be ejected as the atom relaxes; this is shown in Fig. 4.5 for noble gases. Formulae for specific cases, and a wealth of experimental data can be found in: Bambynek, et al., (1972), Rev. Mod. Phys. 44, 716; and Chattarji (1976), "Theory of Auger Transitions.".

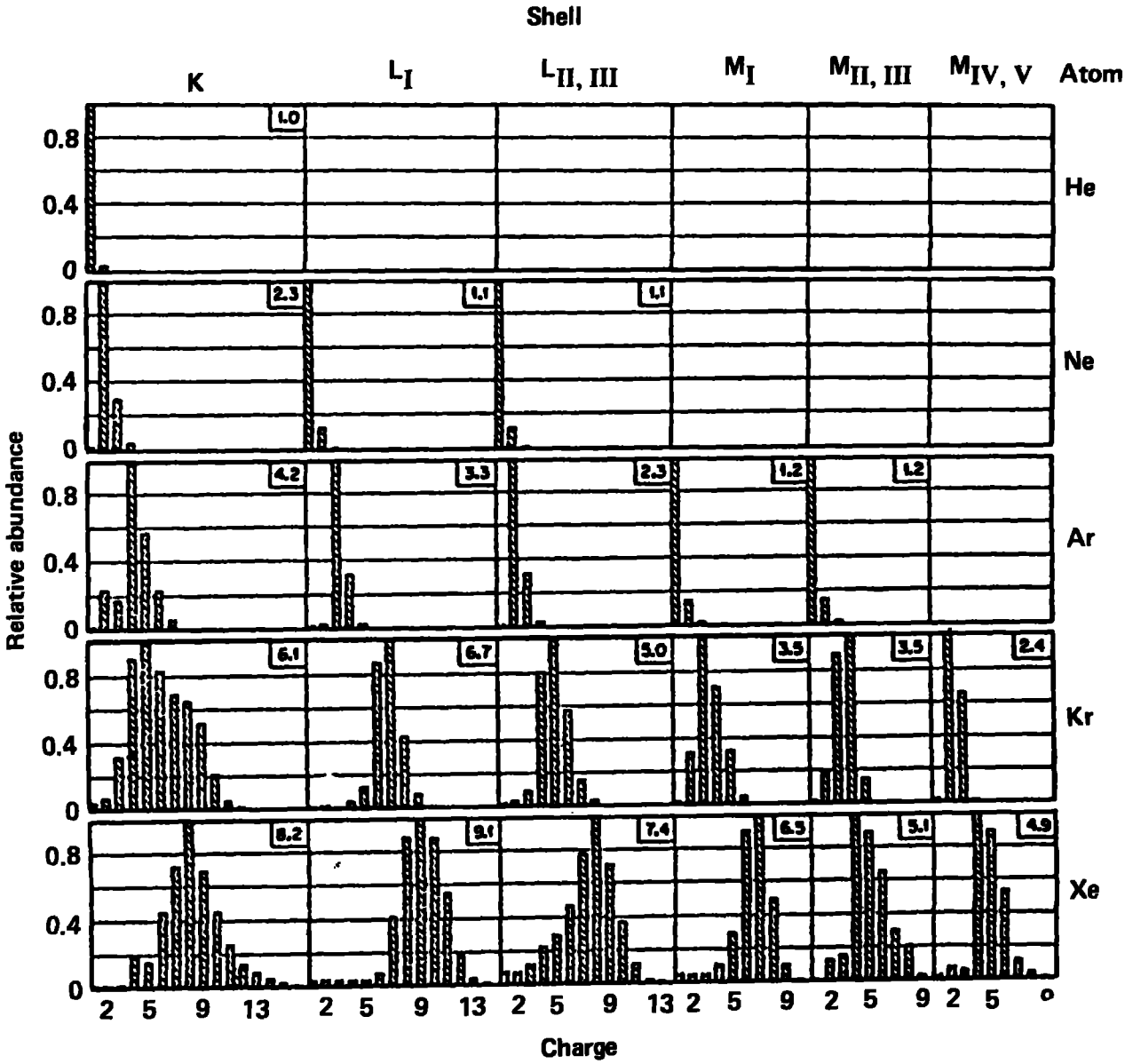

FIG. 4.5. The relative abundances of ions that are formed as the consequence of a sudden vacancy in the K, L, and M shells of the rare gases. The average charge is given for each spectrum in the upper right-hand corner. The bars containing a notch on top represent an upper limit to the designated intensity. [Figure from Carlson et al. (1966), Phys. Rev. 151, 41.]

Numerical values for probabilities of autoionization typically range from 10^{13} sec^{-1} to 10^{14} sec^{-1}, and for a given transition the scaling with nuclear charge is weak,

$$W^{(a)}(Z) \sim Z^{s} W^{(a)}(1), \quad 0 \leq s \leq 1/2 \ . \tag{4.28}$$

Because these transition probabilities are so large, it is very seldom that other processes (collisional or radiative) can interfere with the internal re-arrangement of an atom that finds itself with an inner-shell vacancy.

Collisional Excitation-Autoionization

It is now easy to understand that excitation of an inner electron can lead to auto-ionization. Until recently, though, it was throught that such a process is unlikely, and so it was not included in calculations of collisional ionization rates. Within the last few years, experiments at ORNL and JILA have shown this expectation to be wrong: inner-shell excitation, followed by autoionization can increase the total ionization rate by as much as a factor of 10! Figures 4.6 and 4.7 reproduce some of these data. Information available now suggests that excitation-autoionization becomes increasingly more important as one goes to higher charge states. However, there is too little known at present to even propose Z-scaling behavior.

In principle, there is an inverse to the process of excitation-autoionization: resonant capture followed by de-excitation. This sequence is discussed next.

Resonant Capture

This is the inverse of autoionization, and for the simple example of a Li-like atom one would have

$$e^{-} + Li^{+}(1s^{2}) \rightarrow Li(1s\ 2pn\ell) \ , \ n \geq 2 \ .$$

No radiation is emitted this capture process which, according to the energy level scheme in Fig. 4.4 requires a free electron with only slightly less energy than the $Li^{+}(1s \rightarrow 2p)$ excitation energy. In order to obtain a thermal rate coefficient, it is most convenient to use a thermal balance relation,

$$N_e N(Z+1, \Gamma') C^{(res)}_{\Gamma_d \Gamma'} = N(Z, \Gamma_d) W^{(a)}_{\Gamma' \Gamma_d} \ , \tag{4.29}$$

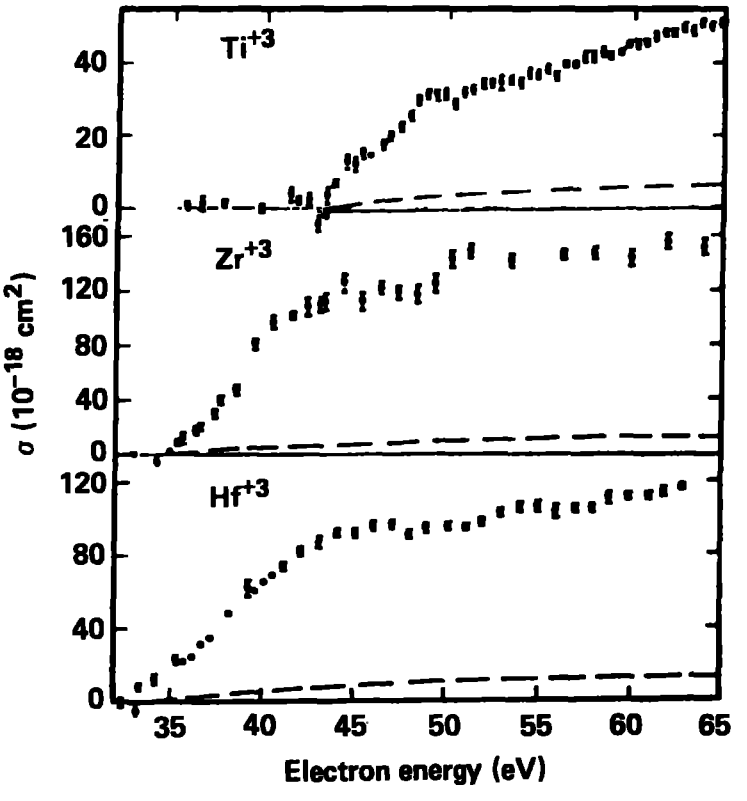

FIG. 4.6. Experimental results for electron impact ionization of Ti^{+3}, Zr^{+3}, and Hf^{+3}. Error bars are one standard deviation of the mean statistical uncertainty. The dashed line is from the semiempirical formula of Lotz. [Figure from Falk et at. (1981), Phys. Rev. Lett. 47, 494.]

plus the Saha equation. Together they yield the general expression

$$C^{(res)}_{\Gamma_d\Gamma'}(T_e) = \frac{g(Z,\Gamma_d)}{2g(Z+1,\Gamma')}\left(\frac{2\pi\hbar^2}{m_e k_B T_e}\right)^{3/2} W^{(a)}_{\Gamma'\Gamma_d}\exp\left(\frac{-\Delta E}{k_B T_e}\right), \qquad (4.30)$$

where $\Delta E>0$ is the energy of the state Γ_d with respect to that of Γ'. To a good approximation, one can replace ΔE by excitation energy corresponding to the transition undergone by the initially-bound electron, e.g., in the example above, $\Delta E \simeq E(Li^+,1s2p) - E(Li^+,1s^2)$. It is particularly important to realize that, in general, Γ_d is a doubly-excited state of the ion "Z".

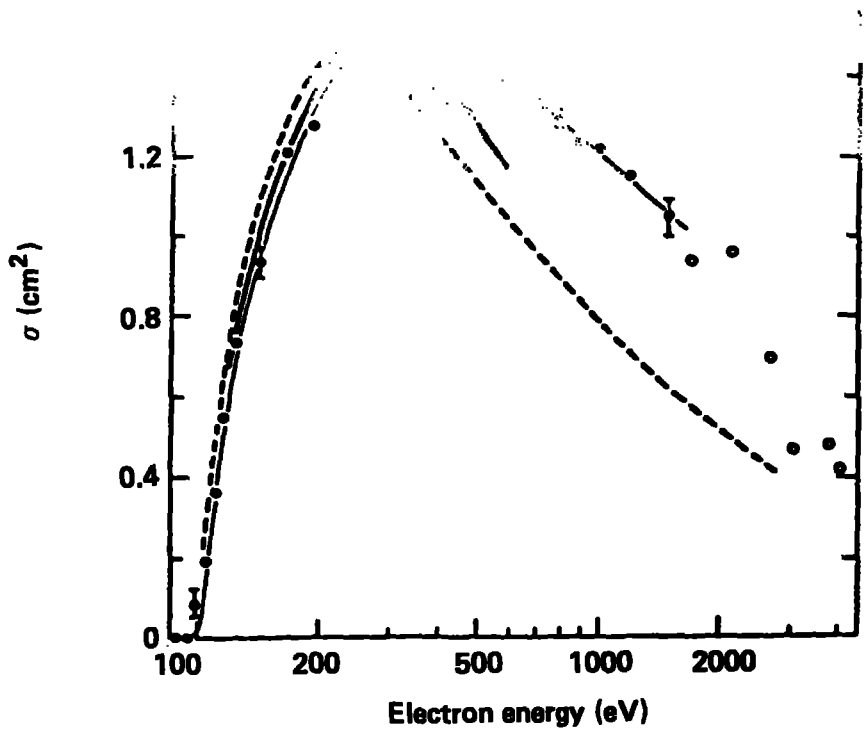

FIG. 4.7. Cross section for electron impact ionization of N^{4+}. The connected full circles are data of Crandall et al., (1979), J. Phys. B12, L249; open circles are data of Donets and Ovsyannikov; broken curve is scaled Coulomb–Born of Golden and Sampson; full bold curve is Coulomb–Born by Moores. [Figure from Crandall et al. (1979).]

Dielectronic Recombination

Although resonant capture does constitute an electron–ion recombination, the autoionization of the newly–formed system usually is so rapid that the net effect is that nothing has happened. But, there is a small chance that the doubly–excited state will stabilize via a radiative or collisional decay before autoionization occurs. When this happens, "dielectronic" recombination has taken place. Only at very high densities would collisional stabilizations be important, and we will not consider their effects here.* We note, however, that collisional stabilizations do represent the inverse of excitation–autionization.

* For a discussion of dielectronic recombination at high densities, see Weisheit (1975), J. Phys.. B8, 2556.

In the simplest possible case, there is only one radiative decay "channel", say $\Gamma_d \to \Gamma_1$, and only one autoionization "channel," $\Gamma_d \to \Gamma'$. The probability of decay is just the branching ratio

$$A_{\Gamma_1\Gamma_d} \Big/ \left[A_{\Gamma_1\Gamma_d} + W^{(a)}_{\Gamma'\Gamma_d} \right] ,$$

and so the rate coefficient for dielectronic recombination via the sequence $\Gamma' \to \Gamma_d \to \Gamma_1$ is

$$\beta^{(diel)}_{\Gamma_1\Gamma_d\Gamma'} = C^{(res)}_{\Gamma_d\Gamma'} \cdot A_{\Gamma_1\Gamma_d} \Big/ \left[A_{\Gamma_1\Gamma_d} + W^{(a)}_{\Gamma'\Gamma_d} \right] . \tag{4.31}$$

Thus, the recombined ion is stabilized in the excited state Γ_1.

Again, using the Li-ion to provide a concrete example, one dielectronic sequence is

$$\underbrace{Li^+(1s^2) + e^-}_{\Gamma'} \quad \to \quad \underbrace{Li(1s2pn\ell)}_{\Gamma_d} \quad \to \quad \underbrace{Li(1s^2 n\ell) + \hbar\omega}_{\Gamma_1}$$

Incidentally, the stabilizing radiative transition $\Gamma_d \to \Gamma_1$, which takes place in the ion (Z) and in the presence of another excited electron, gives rise to what is called a "satellite" of a line in the ion (Z+1). (Here, a satellite of the resonance line $1s2p \to 1s^2$). These lines can be useful for plasma diagnostics.

The total rate of dielectronic recombination for a complex ion is given by a generalization of formula (4.31), in which individual A- and $W^{(a)}$- values are replaced by total decay and autoionization probabilities:

$$\beta^{(diel)}_{\Gamma'}(T_e) = \frac{4a_o^3}{g(Z+1, \Gamma')} \left(\frac{\pi I_H}{k_B T_e} \right)^{3/2} \sum_d e^{-\Delta E/k_B T_e} \; g(Z, \Gamma_d) \; W^{(a)}_{\Gamma'\Gamma_d}$$

$$\cdot \left[\frac{\sum_1 A_{\Gamma_1\Gamma_d}}{\sum_{"} W^{(a)}_{\Gamma"\Gamma_d} + \sum_1 A_{\Gamma_1\Gamma_d}} \right] \tag{4.32}$$

Because of the exponential factor in the resonant capture coefficient, dielectronic recombination usually is not important if $k_B T_e \leq \frac{1}{10} \cdot$ (smallest E1 transition energy). However, at high temperatures, it usually exceeds the rate of radiative recomination. Figure 4.8, taken from A. Burgess' historic paper (1964, Astrophys. J. 139, 776), illustrates this point for He^+. These curves cross at a temperature $k_B T = 0.13\ \Delta E$ (1s, 2p).

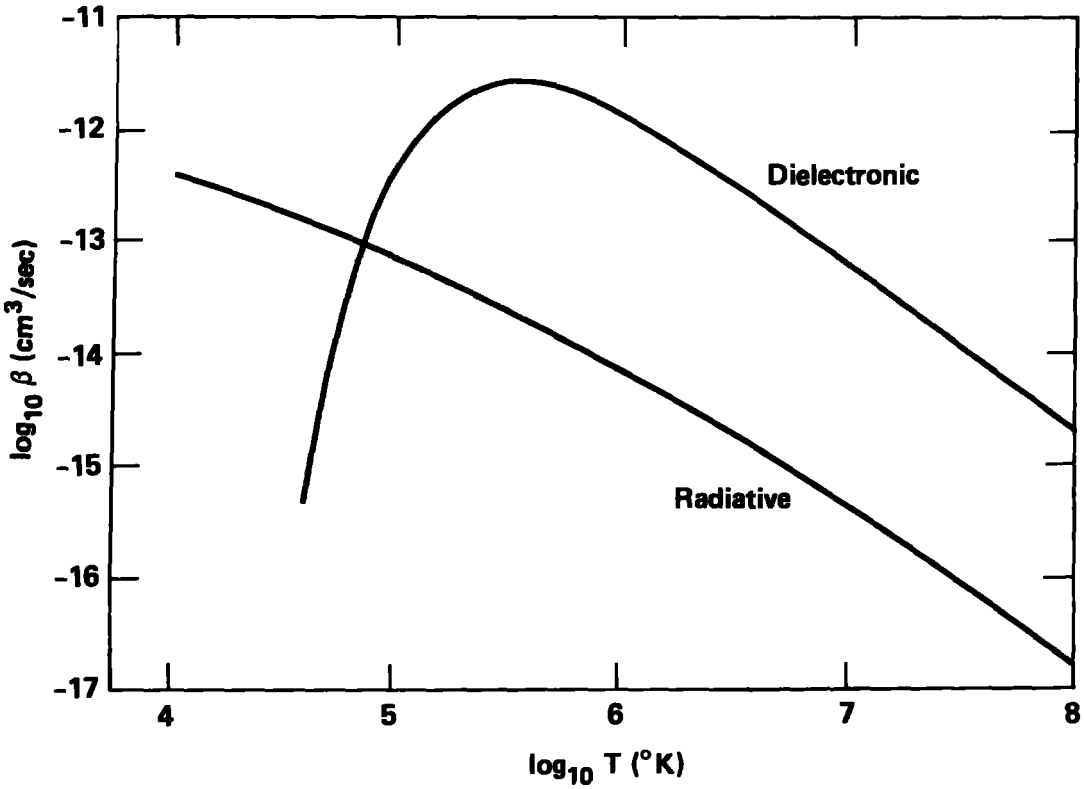

FIG. 4.8. $He^+ + e$ recombination rate coefficients β.

By using hydrogenic wavefunctions, Burgess was able to obtain an approximate formula for the total dielectronic rate coefficient of low-Z ions ($Z \leq 20$). It is

$$\text{BURGESS}\quad \beta^{(diel)} = 4.8 \times 10^{-11} \left(\frac{I_H}{k_B T_e}\right)^{3/2} B(Z+1) \sum_m f_{m1} \mathcal{A}(x_m)\, e^{-\Delta E_{m1}/\gamma k_B T_e}\ \frac{cm^3}{sec}, \qquad (4.33)$$

where the summation is over singly excited states "m" of the more-ionized ion, and where

$$\left.\begin{aligned} Z+1 &= \text{charge of recombining ion} \\ B(Z) &= Z^{1/2}(Z+1)^{5/2} / (Z^2 + 13.4)^{1/2} \\ \mathcal{A}(x) &= x^{1/2}/(1+0.105x + 0.0150x^2) \\ x_m &= \Delta E_{m_1}/(Z+1) \\ \gamma &= 1.0 + 0.015\, Z^3/(1+Z)^2 \quad . \end{aligned}\right\} \qquad (4.34a)$$

In the mid-seventies, A. Merts of LASL pointed out that this expression is reasonably accurate (~ factor 2) for recombinations in which the least energetic excitation of the

already–bound electron does not involve a change of quantum number, a so–called "$\Delta n=0$" case. For "$\Delta n\neq 0$" cases, Merts recommended, instead of the formula $\mathcal{A}(x)$ in Eq. (4.34a), the formula

$$\mathcal{A}'(x) = 0.5\, x^{1/2} / (1 + 0.210x + 0.030x^2) \ . \tag{4.34b}$$

With this modification, the general result is known as the "Burgess–Merts" formula. It has been found recently that, for Z~30, the Burgess–Merts formula does not accurately represent the recombination involving individual stabilizing transitions, m→1. However, the total rates, summed over m–values, are fairly accurate. Whether it works at all for very high ionic charges is unknown.

For cases where the predominant stabilizing radiative decay ($\Gamma_d \rightarrow \Gamma_1$) involves a change of principal quantum numbers of the inner electron ($\Delta n\neq 0$ cases) some scaling properties of the dielectronic rate coefficient can be extracted from the general dependences

$$A \simeq Z^4 10^8 \ \mathrm{sec}^{-1}, \quad W^{(a)} \simeq (Z^6/n^3)\, 10^{14} \ \mathrm{sec}^{-1}, \quad g(Z,n) \sim n^2 \ . \tag{4.35}$$

Here, n is the principal quantum number of the outer electron in the doubly–excited state. Putting these results into the simple expression (4.31) shows that dielectric captures into level n are roughly proportional to

$$\beta_n^{(\mathrm{diel})} \propto \frac{Z^4\, n^2}{1 + n^3 (Z/30)^4} \ , \tag{4.36}$$

which peaks at $n = \tilde{n} \simeq (35/Z)^{4/3}$. As is evident from Fig. 4.9 (for He–like ions), for high–Z ions only states belonging to low n–values need to be considered, but for low Z ions hundreds of levels need to be considered. No wonder tables of rate coefficients are sparse!

The inverse of dielectronic recombination — as discussed here — is the two–step process of photoexcitation – autoionization. To date, no one has investigated problems in which the intensity of radiation is sufficient to warrant the inclusion of this process. Indeed, it is likely that such an intense radiation field would fully ionize a plasma very quickly.

The study of dielectronic recombination is particularly active now. The first experimental data – all for low–Z ions – have just become available in 1983; and several major computational efforts have been launched within the past three years. An excellent review of the field prior to 1980 was given by Dubau and Volonté (1980, Rept. Progress. Physics 43, 199).

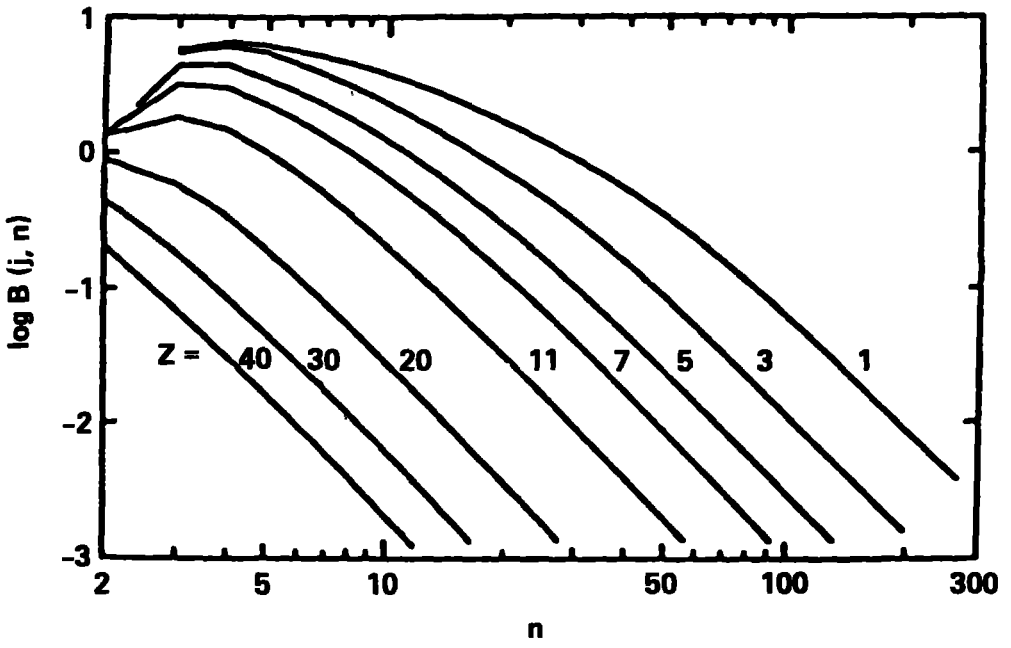

FIG. 4.9. n–dependence of He–like ion dielectronic recombination rate coefficients ($Z=1 \rightarrow He^{+}$).

Ionization Equilibrium

All of the processes we have just described can affect the ionization balance in a plasma. Fortunately, one usually can disregard some of them in any given situation. For steady–state problems, i.e., those in which ionization balance is time–independent, there are three well–defined equilibria that occur in the absence of radiation:

- "coronal equilibrium" – a function of T_e only, and valid only at low densities:

  collisional ionization = (radiative + dielectronic) recombination (4.37)

- "collisional–radiative equilibrium" – a function of T_e and N_e, and appropriate to intermediate densities:

  collisional ionization = (radiative + dielectronic + 3–body) recombination (4.38)

- "collisional equilibrium" – a function of T_e and N_e, and valid only at high densities:

  collisional ionization = (3–body) recombination (4.39)

For plasmas in which ionization is predominantly due to a radiation field, one has a fourth case:

- "photoionization equilibrium" – a function of T_e, N_e, and U_ω, and valid only at low densities:

photoionization = (radiative + dielectronic) recombination (4.40)

Plasmas in photoionization equilibrium are common in astronomy (interstellar gas, quasars, planetary nebulae), and for a discussion of the basic physics see Osterbrock (1974), "Astrophysics of Gaseous Nebulae". Plasmas in thermal equilibria are discribed by the Saha–Boltzman equation.

The most complete study of coronal equilibria is by Post et al. (1978), At. Data & Nuclear Data Tables, 20, 397. Their charge–state distribution of iron is reproduced in Fig. 4.10. Figure 4.11 also pertains to the coronal equilibrium model. It shows, as a function of nuclear charge and electron temperature, the predominant ground–state configuration. For example, at 1 keV, there are still a few 3d electrons bound to element #47 (silver).

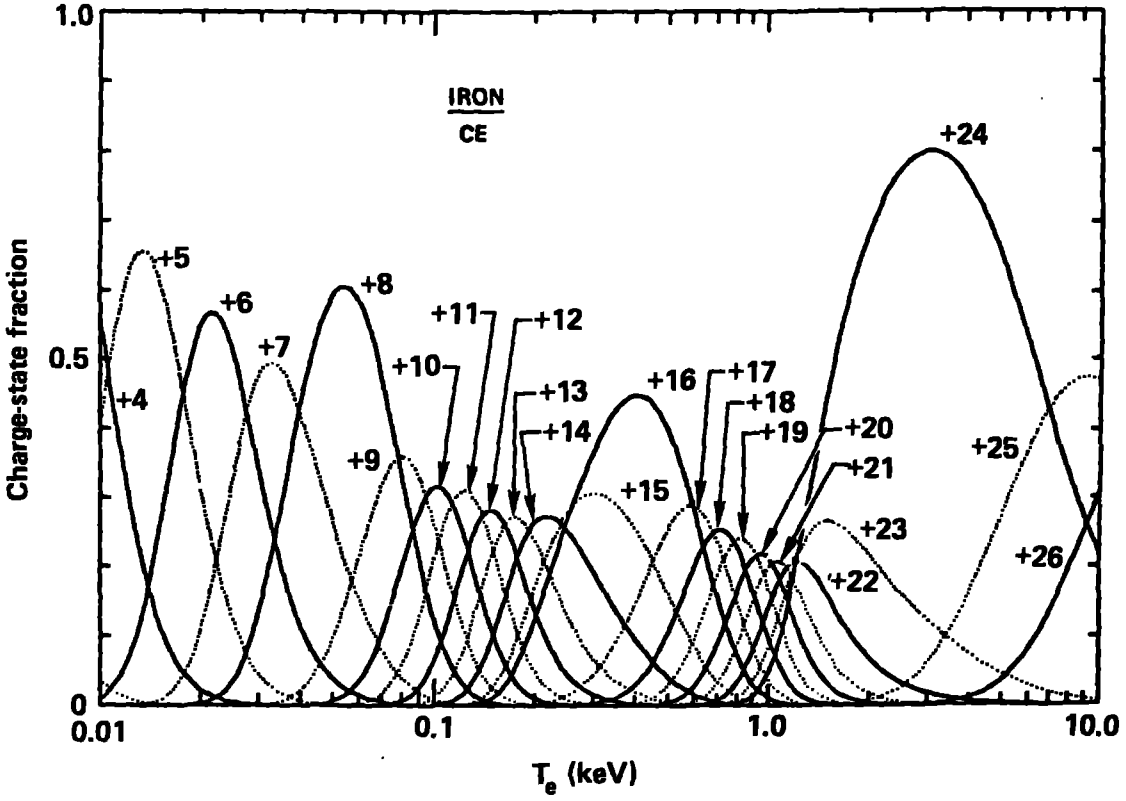

FIG. 4.10. Coronal equilibrium of iron. (Figure courtesy of R. Hulse, Princeton PPL.)

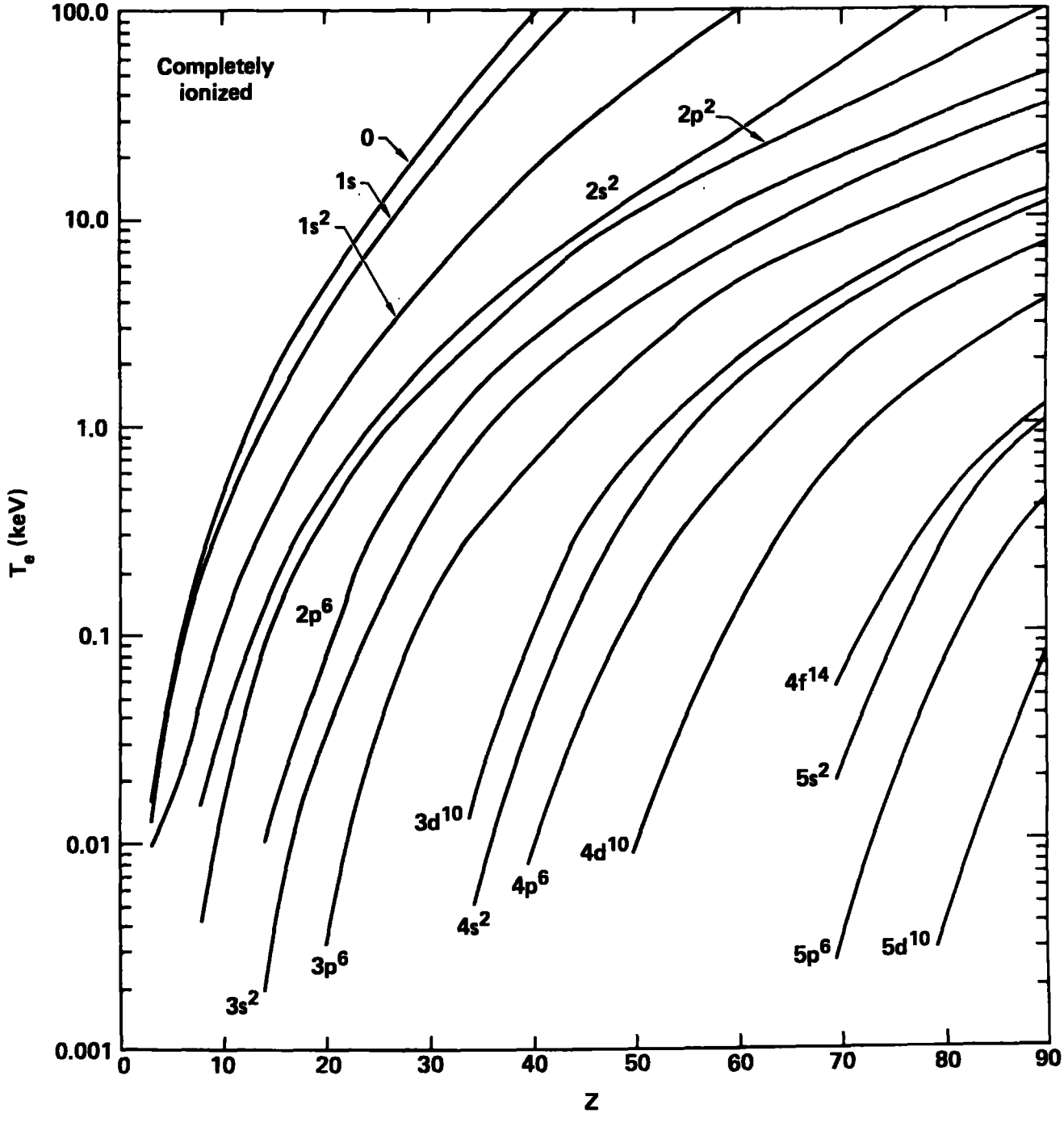

FIG. 4.11. Temperature at which each closed subshell configuration of an element Z is predominant, in coronal equilibrium plasma. (Figure courtesy of D. Post, Princeton PPL.)

The collisional–radiative model was first discussed by Bates, et al., (1962), Proc. Royal Soc. (London), A267, 292, for hydrogenic systems. For this equilibrium, one defines effective ionization and recombination rate coefficients that include all of the cycling of electrons through excited states. Thus,

$$\frac{N_{Z+1}}{N_Z} = \frac{\text{effective ionization rate coefficient}}{\text{effective recombination rate coefficient}} \quad . \tag{4.41}$$

High and low density limits of the effective recombination rate coefficient computed by Bates et al., are reproduced in Fig. 4.12.

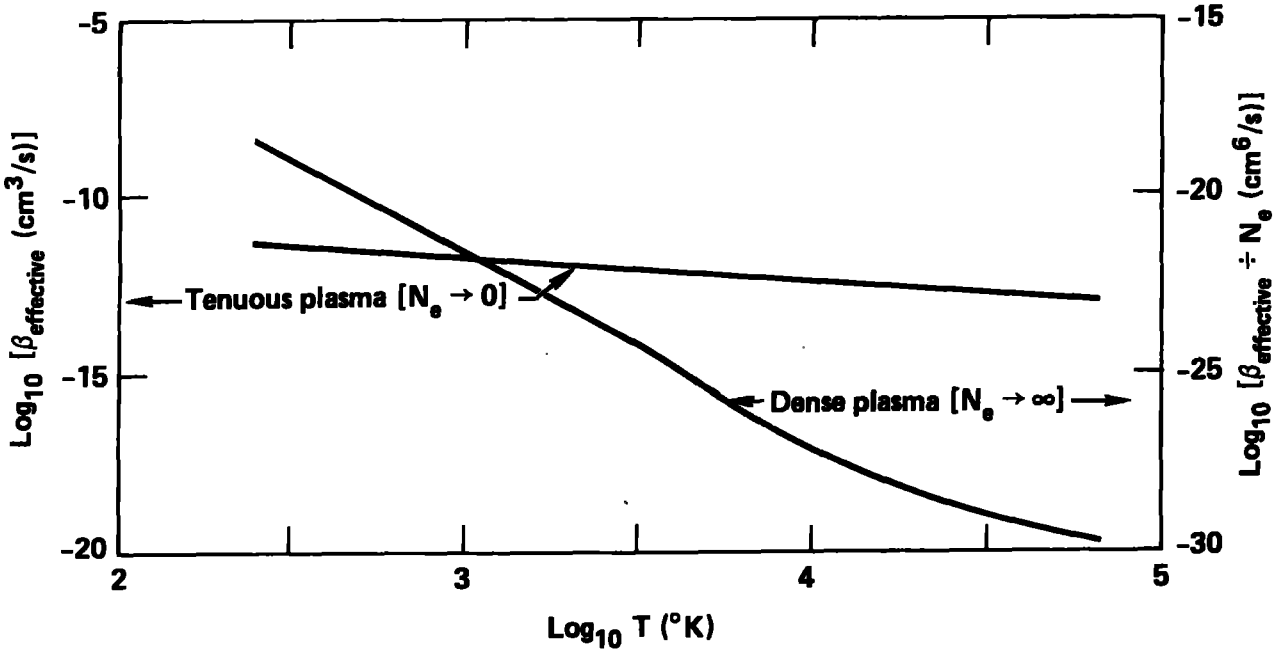

FIG. 4.12. Variation with temperature of the effective recombination rate coefficient β, in the limits of high and low electron density N_e. [Figure from Bates et al. (1962).]

Spectral Line Shapes

Although we have been treating atomic transition energies as being precisely the difference of two eigenvalues, spectral lines are not monochromatic. There is a minimum uncertainty,

$$\delta E_\Gamma \geq \hbar/\tau_\Gamma \ , \tag{4.42}$$

in every excited-state eigenvalue, owing to the state's finite lifetime in vacuo:

$$\tau_{\Gamma} = \left[\sum_{\substack{\text{lower} \\ \text{states}}} A_{\Gamma'\Gamma} \right]^{-1} \quad . \tag{4.43}$$

By analogy with Larmor's treatment of a classical, damped harmonic oscillator, one finds that the distribution of intensity within a spectral line is given by the Lorentz formula

$$I_L(\omega)\, d\omega = \left(\frac{\gamma_{rad}}{2\pi}\right) \cdot \frac{d\omega}{(\omega-\omega_o)^2 + (\gamma/2)^2} \, , \tag{4.44}$$

where $\omega_o = \Delta E/\hbar$ is the central frequency for the transition $\Gamma \rightarrow \Gamma'$, and where

$$\gamma_{rad} = \tau_{\Gamma}^{-1} + \tau_{\Gamma'}^{-1} \tag{4.45}$$

is termed the radiation width of the line; it corresponds to the classical oscillator's damping constant. Here, and in what follows the normalization is $\int I(\omega)d\omega = 1$.

For an emitting gas at a finite temperature, motions of radiating ions give rise to Doppler broadening, which by itself produces a Gaussian line shape,

$$I_D(\omega)\, d\omega = \exp\left[-\left(\frac{\omega-\omega_o}{\Delta\omega_D} \right)^2 \right] \frac{d\omega}{\Delta\omega_D \sqrt{\pi}} \, , \tag{4.46}$$

with the Doppler 1/e width being

$$\Delta\omega_D = \left(\frac{\omega_o}{c}\right) \sqrt{\frac{2k_B T}{M_{ion}}} \quad . \tag{4.47}$$

Almost always, these two broadening mechanisms operate completely independently of each other, and so the line profile resulting from their combined action is given by the convolution of (4.44) and (4.46),

$$I(\omega)\, d\omega = \frac{d\omega}{\Delta\omega_D \sqrt{\pi}} \; H\left(\frac{\omega-\omega_o}{\Delta\omega_D} \, , \, \frac{\gamma_{rad}}{2\Delta\omega_D} \right) \, , \tag{4.48}$$

where the Voigt function (cf. Armstrong, 1967, J.Q.S.R.T. 7, 67),

$$H(x,a) = \frac{a}{\pi} \int_{-\infty}^{+\infty} \frac{\exp(-u^2)du}{(u-x)^2 + a^2} \, , \tag{4.49}$$

is itself a function of the displacement from line center, $\omega-\omega_o$, and the so-called Voigt parameter

$$a = \gamma_{rad} / 2\Delta\omega_D \ . \tag{4.50}$$

Figure 4.13 plots the Voigt function for several values of a.

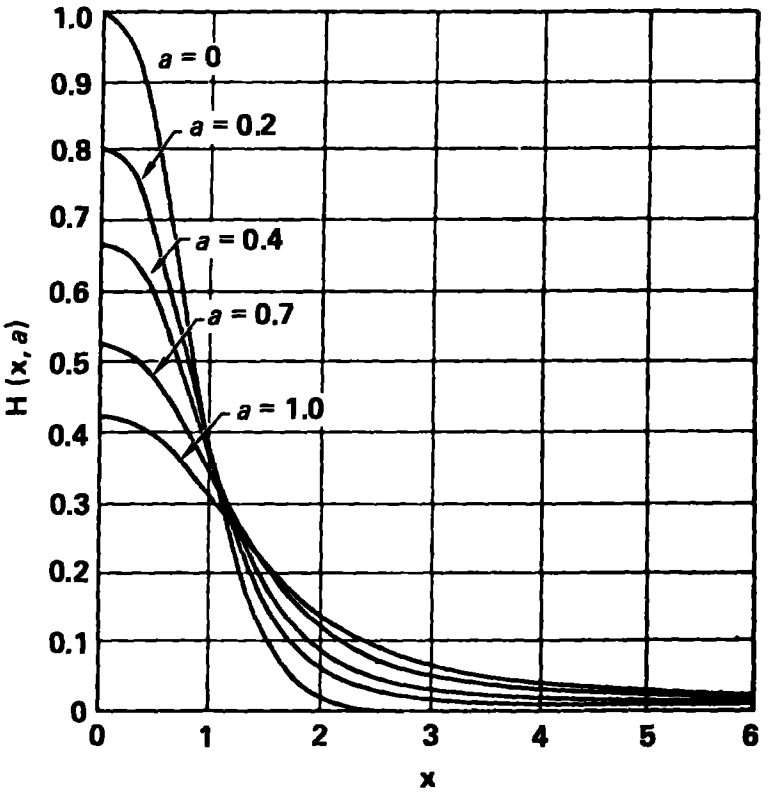

FIG. 4.13. The Voigt function H(x,a). [Figure from Armstrong (1967).]

For plasmas of low density (say, $N_e \leq 10^{14}/cm^3$) the Voigt function, for Doppler and natural broadening, usually constitutes an acceptable description of a line's shape. Unfortunately, in plasmas of even moderate density, the picture is greatly complicated by Stark broadening, which is pressure broadening by charged particles. The central idea is that each ion radiates while "under the influence" of innumerable perturbing ions and electrons. Although elegant theories exist to treat this problem in principle, in practice Stark broadening usually is simplified by two major approximations:

1. Perturbing electrons are treated as abrupt collisional interruptions that change the phase of a radiating ion. If these collisional interruptions occur with a frequency

$$\gamma_e = N_e \langle \tilde{Q} v \rangle \ , \tag{4.51}$$

where $\tilde{Q}$ is some effective cross section, then according to Lorentz, one must generalize Eq. (4.44) by putting

$$\gamma_{rad} \rightarrow \gamma_L = \gamma_{rad} + 2\gamma_e \ . \tag{4.52}$$

Refined theories exist to aid in the calculation of γ_e: these theories show that this collisional, or impact, broadening also is accompanied by a shift $\Delta\omega_e$ of the central frequency away from ω_o. Griem's (1974) text, "Spectral Line Broadening by Plasmas," presents a thorough discussion of this topic.

2. Perturbing ions are treated as the source of an electric field,

$$\vec{\mathscr{E}} = \sum_{ions} \vec{\mathscr{E}}_i \ , \tag{4.53}$$

that is nearly static on timescales $\sim 1/\gamma_{rad}$. This microscopic field shifts and mixes levels of the radiating ion. And, because it splits substates having different projection quantum numbers M of the ion's total angular momentum, it gives rise to line broadening too. Hydrogenic ions experience a perturbation in first order (linear Stark effect), while other ions experience a perturbation only in second order. In either case, what is required for the line broadening problem is the distribution $P(|\mathscr{E}|)$ of field strengths $\mathscr{E}$ for the plasma, in order to weight all possible Stark splittings. [For details on this topic the reader is urged to consult the recent paper by Iglesias, et al., (1983), Phys. Rev. A28, 361.] Figure 4.14 shows some $P(\mathscr{E})$ curves for various values of the plasma parameter

$$\Gamma = (Ze^2 / Rk_BT) \ , \tag{4.54}$$

where R, the typical interionic separation, is defined according to $4\pi R^3 N_{ion}/3 = 1$. As Γ increases, the ions in a plasma are forced into a more ordered arrangement, so (because of greater cancellation) the mean field is weaker.

Altogether then, we can expect shapes of spectral lines arising in plasmas to have the form

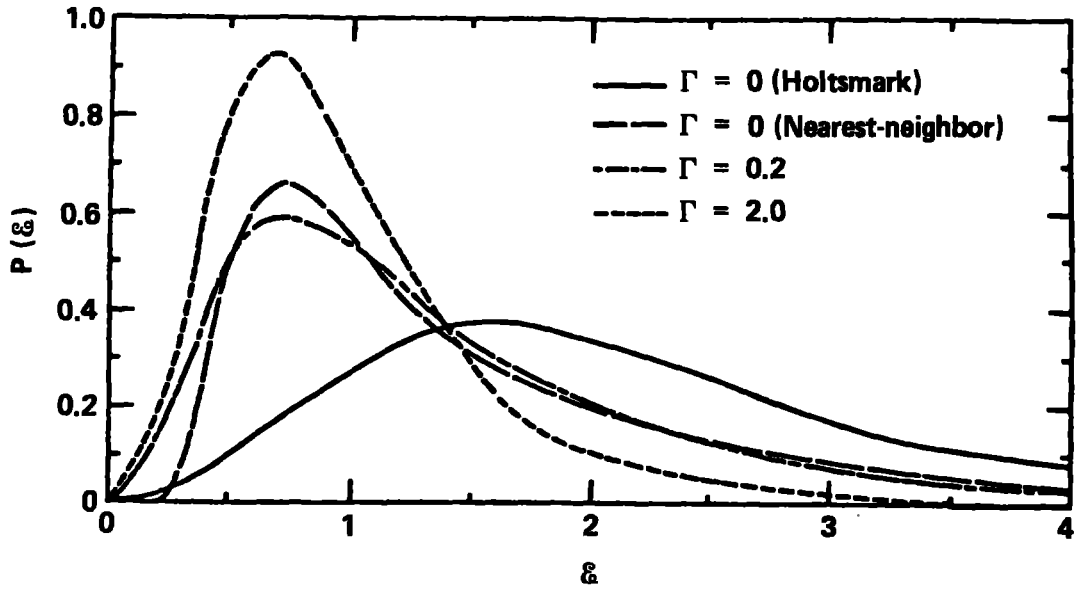

FIG. 4.14. Probability distribution of plasma ion field strengths, measured in units Ze/R^2, for different plasma parameters Γ. The two curves for Γ=0 represent the field of all ions (Holtsmark), and the field of just the nearest-neighbor ion.

$$I(\omega) \sim \sum_{\text{substates}} \int_0^\infty d\mathscr{E} P(\mathscr{E}) H\left[\frac{\omega-\omega_o - \Delta\omega_e - \Delta\omega(\mathscr{E})}{\Delta\omega_D}, \frac{\gamma_L}{2\Delta\omega_D}\right] , \qquad (4.55)$$

where $\Delta\omega(\mathscr{E})$ is the line shift due to the Stark effect. Figure 4.15 shows a calculated plasma-broadened line, under high resolution. The parameters of this He-like Argon plasma correspond to a published laser implosion experiment at the University of Rochester. The details of this calculation are described in the article by Weisheit and Pollock, in "Spectral Line Shapes" (1981).

ACKNOWLEDGMENT

During the past several years, colleagues too numerous to mention individually have encouraged my research on atomic processes in plasmas; during the past year, Joan Balaris has provided expert technical help in the preparation of this manuscript. All these people are sincerely thanked.

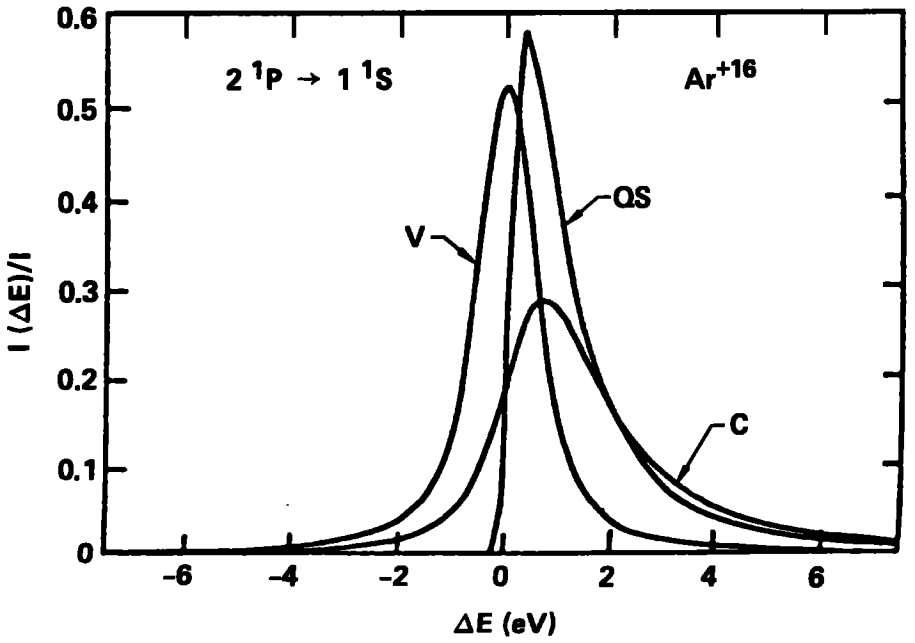

... resonance line, $2^1P \rightarrow 1^1S$, in an 800 eV Ar plasma of density $N_e = 9.6 \times 10^{23}$ cm^{-3}. Curves marked V and QS denote Voigt and quasi-static ion profiles, and that marked C represents their convolution. [Figure from Weisheit and Pollock (1981), "Spectral Line Shapes".]